Schweizerische Eidgenossenschaft
Confédération suisse
Confederazione Svizzera
Confederaziun svizra

Federal Department of the Environment, Transport, Energy and Communications DETEC

Swiss Federal Office of Energy SFOE

Deliverable 3.1, 3.2, and 3.3 dated 06 December 2021

DiGriFlex

D3.1 Pre-scheduling optimization model for distribution grids under uncertainties, and its solution algorithm,
D3.2 On-line optimization model for real-time control/scheduling of controllable resources in a distribution grid, and its solution algorithm,
D3.3 Technical report including the validation of the above optimization models using appropriate test bench and scenarios in a numerical environment.

Date: 6 December 2021

Location: Bern

Subsidiser:
Swiss Federal Office of Energy SFOE
Energy Research and Cleantech Section
CH-3003 Bern
www.bfe.admin.ch

Co-financing
Ministry of Education, University and Research, Italy
through the ERA-NET Smart Energy Systems Regsys joint call 2019

Subsidy recipients:
HEIG-VD - Institut IESE
Route de Cheseaux 1, 1400 Yverdon-les-bains

HEIA-FR
Bd. De Pérolles 80, 1700 Fribourg

DEPsys SA
Route du Verney 20, 1070 Puidoux

Authors:
Mokhtar Bozorg, HEIG-VD, mokhtar.bozorg@heig-vd.ch
Mauro Carpita, HEIG-VD, mauro.carpita@heig-vd.ch
Mohammad Rayati, HEIG-VD, mohammad.rayati@heig-vd.ch

Advisor:
Rachid Cherkaoui, EPFL, rachid.cherkaoui@epfl.ch

SFOE project coordinators:
Dr. Michael Moser, michael.moser@bfe.admin.ch

SFOE contract number: SI/501875-01

Summary

In this report, we present two deliverables of project DiGriFlex aiming to “D3.1: Pre-scheduling optimization model for distribution grids under uncertainties, and its solution algorithm”, “D3.2: On-line optimization model for real-time control/scheduling of controllable resources in a distribution grid, and its solution algorithm”, and "D3.3: Technical report including the validation of the above optimization models using appropriate test bench and scenarios in a numerical environment". WP3 is focussed on i) general formulation of the pre-scheduling optimization, ii) general formulation of the real-time optimization, and iii) definition of the optimization requirement and typical scenarios for the validation in WP4. This report is covering the parts i and ii (equivalent to Tasks 3.1 and 3.2) and part ii (equivalent to Tasks 3.3 and 3.4). The formulations of optimization problems of first-level (pre-scheduling) and second-level (on-line) are given. The input and output data of both optimization problems, including the state and decision variables, are introduced. The criteria and the constraints of distribution grid and controllable components (battery energy storage systems (BESSs) and photovoltaic (PV) production systems) are defined. The proper models are selected for optimization problems of both first- and second-levels. For the first-level problem, the setup of two models of stochastic optimization and distributionally robust optimization (setup of objective and constraints) are introduced complying with uncertainty, in accordance with outcome of WP2. For the second-level, the objective/constraints of the problem are written. According to the nature of mathematical formulation of both optimization problems, the solution approach is chosen. Finally, an appropriate test bench and scenarios in a numerical environment (in Python using optimization solver Gorubi) is developed for validation of the proposed formulation.

Contents

1 Introduction

1.1 DiGriFlex project description

The DiGriFlex project aims at validating effective forecasting and optimal control algorithms for low-voltage (LV) distribution grids. Two high-level objectives are formulated in the project proposal:

1. “Developing effective forecasting and optimal control methods to ensure efficient and secure operation of distribution grids, as well as flexibility and ancillary service provision from the local LV distribution grids to the upstream medium/high voltage grids under uncertainties”,
2. “Implementing the above forecasting and optimal control methods in a LV test grid”.

The general approach in this project is to combine two layers of optimization: in the pre-scheduling step, an optimal point of operation for all controllable resources is identified. Then, in the real-time, the effective outputs (realized outputs) of all controllable resources can be different from the scheduled values because of the existing uncertainties in the resources and the grid. Therefore, the on-line optimization reduces the deviation between the scheduled and effective outputs of the resources considering the feasibility of the resulted dispatch in the grid.

1.2 WP3 description

WP3 “Development of the rolling optimization framework including the formulation of the first-level (pre-scheduling) and on-line optimization problems” delivers the models of optimal control for provisioning flexibility and ancillary services from LV diction grids to the upstream grids under uncertainties. WP3 consists of four tasks:

- Task 3.1: general formulation of the pre-scheduling optimization,
- Task 3.2: general formulation of the on-line optimization,
- Task 3.3: revisiting and refinement of the optimization tools,
- Task 3.4: definition of the optimization requirement and typical scenarios (i.e., case study and grid operation scenarios) for the validation in WP4.

The next chapter will introduce the detailed contents of each task and its association with the three deliverables planned for this WP.

1.3 Deliverable D3.1 definition

In this deliverable “pre-scheduling optimization model for distribution grids under uncertainties, and its solution algorithm”, the formulation of first-level (pre-scheduling) problem of an active distribution grid is presented for providing flexibilities considering the technical constraints of the resources and the grid. To this end, two approaches of stochastic programming and distributionally robust optimization are introduced. The setup of optimization problem including the objective and the constraints is defined. Finally, the numerical validation and the interface with on-line optimization are given.

1.4 Deliverable D3.2 definition

In this deliverable “on-line optimization model for real-time control/scheduling of controllable resources in a distribution grid, and its solution algorithm”, the formulation of second-level (on-line) problem of an active distribution grid is presented for reducing the deviation between the scheduled and effective outputs of the considered resources and obeying the commands of the upstream grid’s operator.

1.5 Deliverable D3.3 definition

The optimization tools are refined and revisited in this deliverable "technical report including the validation of the above optimization models using appropriate test bench and scenarios in a numerical environment." WP1 and WP2 outcomes are used to update the hours-ahead and real-time formulations. Furthermore, the revisited optimization tools are developed and validated numerically (e.g., Python and Gorubi solver).

A number of scenarios must be generated to account for uncertainties in electricity demand and PV power production capabilities in order to solve the ADN's stochastic optimization problem. The scenarios chosen have a direct impact on the outcome of stochastic optimization and, consequently, the robustness/optimality of the derived solution. However, in previous studies, either the scenarios were not provided or the importance of creating realistic scenarios was overlooked. Realistic scenarios must be concise, that is, brief but comprehensive, in the sense that the number of scenarios must be limited while still capturing the typical operation as well as critical circumstances.

Li et al. conducted a survey of various classes of scenario generation methods for renewable energy systems in [13]. The traditional approach, used in [14] and [15], is based on auto-regressive integrated moving average (ARIMA) forecasting and Monte Carlo sampling based on forecast error standard deviation. As demonstrated in [16] and [17], generating a large enough number of scenarios justifies the solution's robustness. This technique, however, is not scalable for ADNs with a large number of buses and time-steps.

A Markov chain-based technique for generating representative scenarios to solve the proposed stochastic optimization problem of ADN while taking advantage of underlying flexibilities is presented in this report.

A Markov chain-based technique for generating representative scenarios to solve the proposed stochastic optimization problem of ADN while taking advantage of underlying flexibilities is presented in this report.

To address the shortcomings of previous studies, we present a scalable and data-driven optimization problem for scheduling the underlying real and reactive power flexibilities of ADNs. For ADN operators, we devised a stochastic optimization problem. Because of operational uncertainties, the proposed stochastic optimization algorithm takes into account all ADN component constraints as well as security/quality limits (i.e., lines and DERs). Variations in PV system production capability, electricity demand, the request of the external network's operator to deploy the planned flexibilities, and the magnitude of the PCC's voltage are all examples of operational uncertainties. We anticipate a data-driven scenario selection strategy based on measured data for proposed stochastic optimization, resulting in lower computational cost.

2 WP planning

2.1 Project plan

Based on the breakdown of activities presented in the previous chapter, the time plan of WP3 shown in Figure 1 has been established.

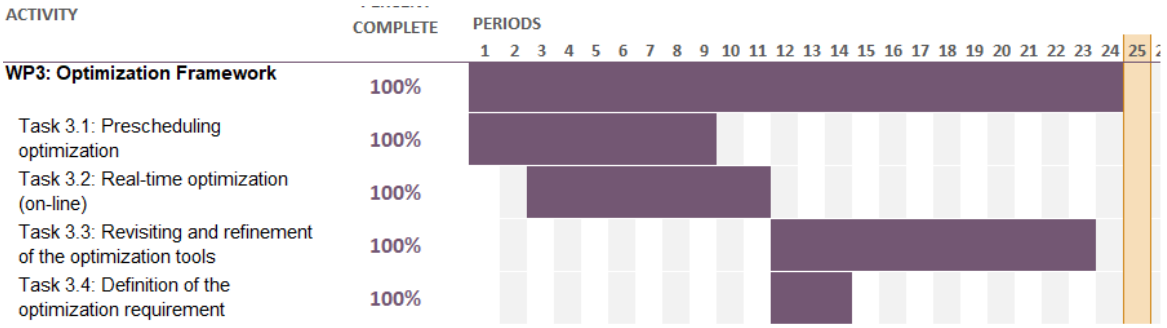

Figure 1: Summary of WP3 time plan

2.2 Tasks description

Figure 1 shows the progress and plan of the proposed tasks in WP3. This report includes the results of tasks 3.1 and 3.2. In the following, the detailed sub-tasks for these two tasks are listed.

Task 3.1: General formulation of the pre-scheduling optimization

- Setup of the electrical model of the grid
- Definition of the input data and the output optimization variables (state variables, decision variables)
- Definition of the criteria and the constraints
- Choice and setup of the appropriate mathematical formulation (objectives and constrains) complying with uncertainty, in accordance with the outcomes of WP2
- According to the mathematical formulation nature, choice of the solution approach
- Setup the interface with on-line optimization
- Development/Validation using appropriate test bench and scenarios in a numerical environment

Task 3.2: General formulation of the on-line optimization

- Definition of the input data and the output optimization variables (state variables, decision variables)
- Definition of the criteria and the constraints
- Choice and setup of the appropriate mathematical formulation (objectives and constrains) complying with uncertainty and real-time requirements, in accordance with the outcomes of WP2
- According to the mathematical formulation nature, choice of the solution approach
- Development/Validation using appropriate test bench and scenarios in a numerical environment

Task 3.3: Revisiting and refinement of the optimization tools

- Update the hours ahead formulation according to WP1 and WP2 outcomes
- Update the real-time formulation according to WP1 and WP2 outcomes
- Development and validation of the revisited optimization tools in a numerical environment (e.g., Python)

Task 3.4: Definition of the optimization requirement and typical scenarios (i.e., case study and grid operation scenarios) for the validation in WP4

2.3 Notations

The main notations are defined in the following. Other symbols are defined as needed throughout the text.

- Indices:

n	Index of buses.
i	Index of PVs.
s	Index of BESSs.
d	Index of demands.
t	Index of time-periods.
f	Index of flexibility services, i.e., $f \in \{P+, P-, Q+, Q-\}$; $P+, P-, Q+, Q-$ represent upward active power flexibility, downward active power flexibility, upward reactive power flexibility, and downward reactive power flexibility.
ω	Index of scenarios of uncertain parameters.

- Sets:

$\mathbb{N}$	Set of buses/nodes.
$\mathbb{N}^{(TC)}$	Set of connection nodes of distribution grid to the upper layer grid.
Θ_n	Set of nodes connected to sending node n.
I	Set of all PVs; I_n is the set of PVs at node n.
S	Set of all BESSs; S_n is the set of BESSs at bus n.
D	Set of demands; D_n is the set of demands at node n.
T	Set of all time-periods in scheduling problem.
Ω	Set of scenarios of uncertain parameters.
$\mathbb{C}$	Complex numbers set.
$\mathbb{R}$	Real numbers set.

- Variables:

$V_{nt\omega}$	Voltage phasor of node n, time period t, and scenario ω [V].
$\lvert V_{nt\omega} \rvert$	Voltage magnitude of node n, time period t, and scenario ω [V].
$I_{nn't\omega}$	Current phasor of line from node n to node n', time period t, and scenario ω [A].
$\lvert I_{nn't\omega} \rvert$	Current magnitude of line from node n to node n', time period t, and scenario ω [A].
$\delta_{nt\omega}$	Voltage phase angles of node n, time period t, and scenario ω [rad].
$P_{nt\omega}$	Active power injection of node n, time period t, and scenario ω [W].
$Q_{nt\omega}$	Reactive power injection of node n, time period t, and scenario ω [Var].
$P_{nn't\omega}$	Active power flow of line from node n to node n', time period t, and scenario ω [W].
$Q_{nn't\omega}$	Reactive power flow of line from node n to node n', time period t, and scenario ω [Var].
$v_{nt\omega}$	Squared voltage magnitude of node n, time period t, and scenario ω; $v_{nt\omega} = \lvert V_{nt\omega} \rvert^2$ [V^2].

$l_{nn't\omega}$ Squared magnitude of current flow of line from node n to node n', time period t, and scenario ω [A].

$P_{it\omega}^{(PV)}$ Active power output of PV production system i for time period t, and scenario ω [W].

$Q_{it\omega}^{(PV)}$ Reactive power output of PV production system i for time period t, and scenario ω [Var].

$P_{dt\omega}^{(DEM)}$ Active power consumption of demand d for time period t, and scenario ω [W].

$Q_{dt\omega}^{(DEM)}$ Reactive power consumption of demand d for time period t, and scenario ω [Var].

$\mathrm{SOC}_{st\omega}$ Energy content of the BESS s in time step t, and scenario ω [Wh].

$P_{st\omega}^{(BESS)}$ Power used to charge (discharge, if negative) the BESS s in time step t, and scenario ω [W].

$Q_{st\omega}^{(BESS)}$ Injected reactive power of the BESS s in time step t, and scenario ω [W].

$P_{nt}^{(SC)}$ Offered active power for injecting to the upper layer grid at connection node $n \in \square^{(TC)}$ and time t [W].

$Q_{nt}^{(SC)}$ Offered reactive power for injecting to the upper layer grid at connection node $n \in \square^{(TC)}$ and time t [Var].

$P_{nt\omega}^{(RT)}$ Produced active power for injecting to the upper layer grid at connection node $n \in \square^{(TC)}$ and time t [W].

$Q_{nt\omega}^{(RT)}$ Produced reactive power for injecting to the upper layer grid at connection node $n \in \square^{(TC)}$ and time t [Var].

$R_{nt}^{(SC,f)}$ Offered flexibility service f for injecting to the upper layer grid at connection node $n \in \square^{(TC)}$ and time t [W or Var].

$r_{nt\omega}^{(RT,P/Q)}$ Deployed active/reactive power flexibility at connection node $n \in \square^{(TC)}$ and time t, and scenario ω [W or Var].

$\alpha_{it}^{(PV,f)}$ Participation factor of PV systems [W or Var].

$\alpha_{st}^{(BESS,f)}$ Participation factor of BESSs [W or Var].

$\alpha_{st}^{(RT,f)}$ Participation factor of power injections at connection point in real-time [W or Var].

- Parameters:

$|\mathbb{N}|$ Number of buses.

$|\mathrm{T}|$ Number of time-steps in scheduling optimization problem.

$|V_n^{(min)}|$ Minimum voltage limit of node n [V].

$|V_n^{(\max)}|$ Maximum voltage limit of node n [V].

$|I_{nn'}^{(max)}|$ Maximum current limit of line from node n to node n' [A].

$\mathrm{Y}_{nn'}$ Admittance of line from node n to node n' [mho].

$\mathrm{G}_{nn'}$ Conductance of line from node n to node n' [mho].

$\mathrm{B}_{nn'}$ Susceptance of line from node n to node n' [mho].

$\mathrm{r}_{nn'}$ Series resistance of line from node n to node n' [ohm].

$\mathrm{x}_{nn'}$ Series inductance of line from node n to node n' [ohm].

$K_{nn'}^{(VP)}$ Sensitivity factor $\partial|V_n|/\partial P_{n'}$ [V/W].

$K_{nn'}^{(VQ)}$ Sensitivity factor $\partial |V_n| / \partial Q_{n'}$ [V/Var].

$K_{nn'n''}^{(IP)}$ Sensitivity factor $\partial |I_{nn'}| / \partial P_{n''}$ [V/W].

$K_{nn'n''}^{(IQ)}$ Sensitivity factor $\partial |I_{nn'}| / \partial Q_{n''}$ [V/Var].

$\mathrm{SOC}_{st\omega}$ Energy content of the BESS s in time step t, and scenario ω [Wh].

$\gamma_s^{(LV)}$ Leakage rate of BESS s as a fraction of state of the charge [%].

$\gamma_s^{(LC)}$ Constant leakage rate of BESS s [%].

$\eta_s^{(D)}$ Discharge efficiency of BESS s [%].

$\eta_s^{(C)}$ Charge efficiency of BESS s [%].

$\mathrm{SOC}_s^{(min)}$ Minimum energy content of BESS s [Wh].

$\mathrm{SOC}_s^{(\max)}$ Maximum energy content of BESS s [Wh].

$S_s^{(BESS,max)}$ Power limit of the BESS s [VA].

$V_i^{(PV,grid)}$ Grid voltage from the viewpoint of PV system i [kV].

$V_i^{(PV,conv)}$ Converter voltage of PV system i [kV].

$X_i^{(PV)}$ Thévenin reactance from the viewpoint of PV system i [kV].

$S_i^{(PV,\max)}$ Maximum power of PV system i based on its converter current limit [VA].

$P_{it\omega}^{(PV,max)}$ Maximum production of PV system i based on available solar irradiance at time period t and scenario ω [W].

$\lambda_{nt}^{(P)}$ Price of active power in scheduling market for time period t and connection point n [CHF/W].

$\lambda_{nt}^{(Q)}$ Price of reactive power in scheduling market for time period t and connection point n [CHF/W].

$\lambda_{nt}^{(f)}$ Price of flexibility service f in scheduling for time period t and connection point n [CHF/W or CHF/Var].

- Vector and Matrices:

$\vec{V}$ Vector of voltage phasors of buses.

$\overrightarrow{|V|}$ Vector of voltage magnitudes of buses.

$\vec{\delta}$ Vector of voltage phase angles of buses.

$\vec{P}$ Vector of active power injections of buses.

$\vec{Q}$ Vector of reactive power injections of buses.

$\mathbf{Y}$ Network admittance matrix.

$\mathbf{G}$ Network conductance matrix.

$\mathbf{B}$ Network susceptance matrix.

$\mathbf{R}$ Network resistance matrix.

$\mathbf{X}$ Network inductance matrix.

3 Setup of the electrical model of the grid

In this project, the two-level rolling optimization framework is presented to ensure optimal (most economic) and secure operation of an active distribution grid under uncertainties. The first-level (pre-scheduling optimization) deals with a time-ahead scheduling (e.g., day-ahead or few hours ahead basis) of the controllable resources, whereas the second-level (on-line optimization) deals with on-line scheduling of the controllable resources.

The objective of pre-scheduling optimization problem is to minimize the relative expected cost of operation with respect to the estimation (forecast) of the uncertain parameters. This objective function includes the balancing cost minus revenues from provisioning ancillary services or any flexibilities to the upstream transmission system. At this level, the main uncertain parameters are the power generation of renewable energy sources (e.g., PV), and power demand of consumers in the coming hours. The pre-scheduling optimization problem is solved one day before the target day (day -1), since we want to determine the participation of active distribution grid in the markets of energy and ancillary services.

The objective of on-line optimization problems is to minimize the deviation of the outputs of controllable resources (e.g., storages) from the pre-scheduled set-points obtained from the first-level, with respect to the real-time realization of the uncertain parameters. In this respect, the on-line optimization relies on a very short-term forecast of uncertain parameters near real-time, which is one of the subjects of WP 2 of this project. Prediction of PV systems outputs and demands in next ten minutes is done in the very short-term forecast system proposed in WP2. The on-line optimization problem is solved ten minutes before the target time step, as the time step is considered equal to 10 minutes in this study. The reason behind selection of ten minutes for time step is that the measurements are captured every 10 minutes in standard distribution systems. However, the market clearance is done every 15 minutes, the participation of active distribution network in the real-time market is not considered in this project.

The two-level rolling optimization problems are linked together through the technical constraints of the grid, as well as the constraints associated with the capacities of the controllable resources (e.g., state of charge limits of the batteries). Moreover, the second-level (on-line) optimization problems will provide deviation feedbacks to the first-level pre-scheduling problem (that will solve for upcoming time windows) to enhance the overall optimality and security of operation of distribution grid operation in a larger time window (e.g., one day). If the deviation from the schedules is more than what expected, some parameters of the first-level optimization problem should be updated. Figure 2, depicts a simple schematic of the proposed optimization framework.

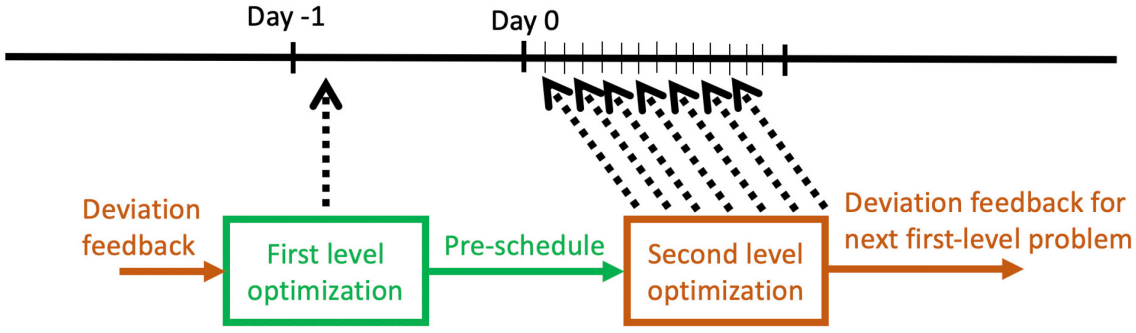

Figure 2: Two-level optimization framework

The optimization problems will be constrained by a) technical limitations of the distribution grids (e.g., voltage limits, power flow limits and so on) and b) capacity and technical limits of controllable resources

(e.g., state of charge of batteries), with respect to the real-time measurements. Moreover, the possibility of supplying ancillary service and flexibility provision (i.e., both voltage and frequency control services) from the distribution grid to the upstream transmission grid is taken into account.

3.1 Definition of the input data and the output optimization variables

3.1.1 Definition of state and decision variables of pre-scheduling optimization

The block diagram of pre-scheduling problem (first-level) is depicted in Figure 3. The pre-scheduling set-points and offers to both energy and flexibilities markets are optimized in the day-ahead scale using a robust optimization problem. For writing this optimization problem, the PV model, including the weather forecast for next 24 hours, is employed. This forecast cannot be 100% accurate; thus, the error of forecast should also be included in the model of optimization problem. In addition, the parameters and forecast of demands are used. Finally, we need the parameters of distribution network to write an optimization problem for maximizing the net income and minimizing the deviation from the schedule in all scenarios of forecasting error. The proposed optimization problem in the pre-scheduling horizon must be robust against the uncertainties of forecasts. As a result, in the case of deviation from the forecast values in the real-time, the resources are optimally controlled to minimize the net deviation; in addition, these deviation experiences are used in the pre-scheduling optimization problem of next days by tuning some parameters of robust optimization (which is explained later on). Thus, this feedback in the model is considered to reinforce the proposed model through the experiences and bi-directional interaction with the environment. It is worth mentioning that in addition to this feedback, a high number of operation scenarios is considered in the formulation of proposed pre-scheduling (first-level) problem for ensuring the dispatch possibility of distribution grid.

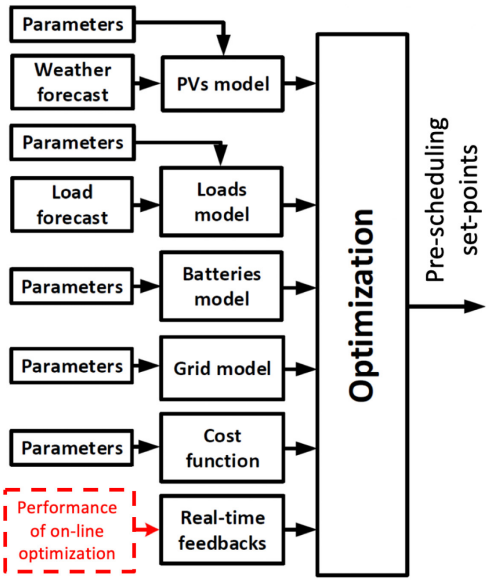

Figure 3: Structure of inputs/outputs of pre-scheduling problem (first-level)

Therefore, the input variables of this pre-scheduling optimization problem are as follows:

- Parameters of PV production systems (grid voltage, converter voltage, and Thevenin reactance), BESSs (charging and discharging efficiencies), distribution grid (resistances and reactance), and voltage magnitude of connection point, i.e., $|V_{nt\omega}|: n \in \mathbb{N}^{(TC)}$.

- Prediction of demands at each time step based on a number of scenarios, i.e., $P_{dt\omega}^{(DEM)}$ and $Q_{dt\omega}^{(DEM)}$.
- Prediction of maximum possible outputs of PV production systems at each time step based on a number of scenarios, i.e., $P_{it\omega}^{(PV,max)}$.
- Cost functions parameters such as $\lambda_{nt}^{(P)}$, $\lambda_{nt}^{(Q)}$, and $\lambda_{nt}^{(f)}: f\{P+, P-, Q+, Q-\}$.
- The asked active and reactive power of upper layer grid operator from the DSO, i.e., $r_{nt\omega}^{(RT,P)}$ and $r_{nt\omega}^{(RT,Q)}$.

The output variables of pre-scheduling problem are as follows:

- Active and reactive power offers to the day-ahead market at the connection nodes ($P_{nt}^{(SC)}$ and $Q_{nt}^{(SC)}$).
- Active and reactive power flexibility services offered to the day-ahead market at the connection nodes ($R_{nt}^{(SC,f)}: \forall f \in \{P+, P-, Q+, Q-\}$).
- Active and reactive power set-points of PVs at each time step and each scenario of operation ($P_{it\omega}^{(PV)}$ and $Q_{it\omega}^{(PV)}$).
- State of charge and active/reactive input powers of BESSs at each scenario of operation ($\mathrm{SOC}_{st\omega}$, $P_{st\omega}^{(BESS)}$, and $Q_{st\omega}^{(BESS)}$).
- Distribution grid variables including square of currents and voltage ($v_{nt\omega}$ and $l_{nn't\omega}$), and all variables related to the exact Distflow model.
- Real-time injections of active/reactive power at connection node, which may deviate from asked active/reactive power by upper layer grid operator based on scheduled flexibilities ($P_{nt\omega}^{(RT)}$ and $Q_{nt\omega}^{(RT)}$).

3.1.2 Definition of state and decision variables of on-line optimization

The block diagram of on-line (second-level) problem is illustrated in Figure 4. In real-time, two operation modes are considered since there is a hierarchy of operation in real-time. Here, the hierarchy is due to the fact that the operation of distribution grid must be continued even the solution of on-line optimization problem is not found. To this end, the default set-point values (the set-point in previous time-step) must be used for set-points of flexible resources in the case that the main optimization problem does not find the global optimal solution. To summarize, these two operation modes are defined in the following:

- Mode 1 or main mode: The main optimization problem for finding the set-points of flexible resources in the distribution network considering the commands of upper layer grid operator or TSO for providing flexibilities is implemented. Note that the command of upper layer grid operator is considered in the pre-scheduling optimization problem with a boundary; however, in real-time, the exact command is known.
- Mode 2: The default values are used when the outputs of mode 1 are not available (if the solution of optimization problem is not determined in the dedicated time). This mode can be used as backup plan for the proposed control system in real-time.

Using mentioned two modes, the hierarchy of proposed control system is kept from the viewpoint of distribution network' operator because the operation of distribution grid is not disturbed in the case that the on-line optimization problem is not solved in the dedicated time. The block of "switch" in Figure 4 decides the activation of each mentioned mode. The rule of this "switch" is as below: if the solution of

mode 1 is not available after a time instant, the outputs of mode 2 (which are the default values) are used as the outputs.

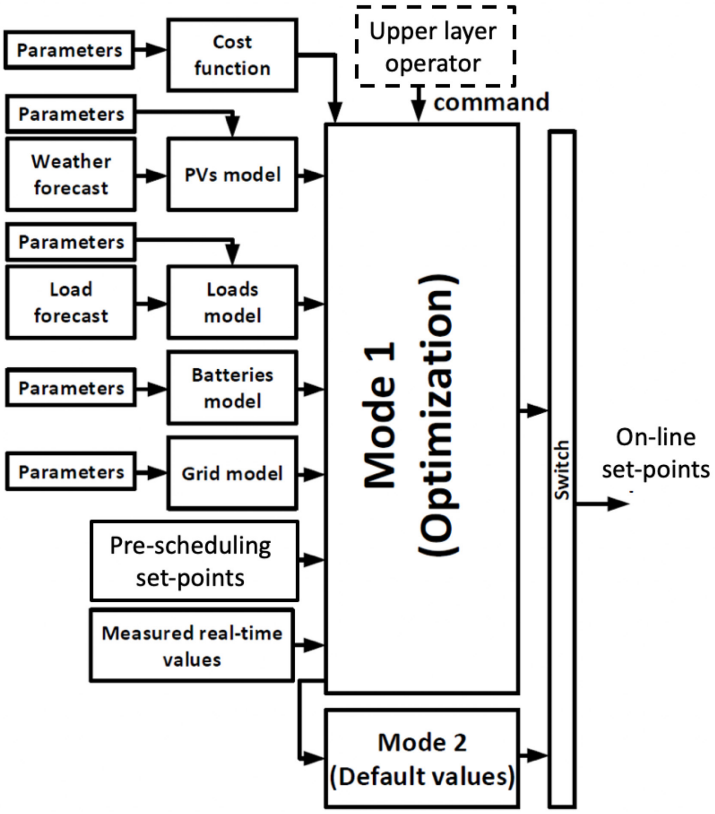

Figure 4: Structure of inputs/outputs of on-line problem (second-level)

Therefore, the input variables of the on-line optimization problem are same as the inputs of pre-scheduling problem. In addition, the outputs of pre-scheduling problem are other inputs of the on-line problem. Finally, the outputs of the on-line optimization problem are as below:

- Active and reactive power set-points of PVs ($P_i^{(PV)}$ and $Q_i^{(PV)}$).
- State of charge or energy content and active/reactive input powers of BESSs (SOC_s, $P_s^{(BESS)}$, and $Q_s^{(BESS)}$).
- Distribution grid variables including square of currents and voltage (v_n and $l_{nn'}$), and all variables related to the exact Distflow model.
- Real-time injections of active/reactive power at connection node, which may deviate from asked active/reactive power by upper layer grid operator based on scheduled flexibilities ($P_n^{(RT)}$ and $Q_n^{(RT)}$).

3.2 Definition of the criteria and constraints

In this section, different models of power flow, capability constraints of battery energy storage systems (BESSs), the capability constraints of PV systems, and the constraints related to the connection point of distribution grid and the upper layer grids are presented.

Here, the distribution grid can refer to the LV grid (with any voltage below 1 kV based on the standard of SwissGrid); then, the upper layer grid would be the medium-voltage grid (with any voltage ranging between 1 kV and 36 kV based on the standard of SwissGrid). However, if the distribution grid refers to the medium-voltage grid itself; then, the upper layer grid would be high-voltage level transmission grid (with voltage ranging between 36 kV and 150 kV based on the standard of SwissGrid).

3.2.1 Constraints of distribution grid

Consider a distribution grid, where n and $\mathbb{N}$ denote the index and set of nodes, respectively. The network admittance matrix, containing the electrical parameters and topology information, is denoted by $\boldsymbol{Y} := \boldsymbol{G} + j\boldsymbol{B}$, where $j := \sqrt{-1}$. Define $(.)^*$ as the complex conjugate.

All presented models in this section are given for a single sequence, one time step, and a scenario. The indices of t and ω (referring to the time-step and scenario, respectively) are dropped here. Based on the requirements and necessities, these indices must be added into the models.

The power flow models are presented to balance the injection and withdrawal power of different buses in the grid. Each bus $n \in \mathbb{N}$ has active and reactive power injections $P_n + j.Q_n$, $\vec{P}, \vec{Q} \in \mathbb{R}^{|\mathbb{N}|}$. The active and reactive power injections of each bus are equal to

$$P_n = \sum_{i \in \mathbb{I}_n} P_i^{(PV)} + \sum_{s \in \mathbb{S}_n} P_s^{(BESS)} - \sum_{d \in \mathbb{D}_n} P_d^{(DEM)}; \quad \forall n \in \mathbb{N}, \tag{1}$$

$$Q_n = \sum_{i \in \mathbb{I}_n} Q_i^{(PV)} + \sum_{s \in \mathbb{S}_n} Q_s^{(BESS)} - \sum_{d \in \mathbb{D}_n} Q_d^{(DEM)}; \quad \forall n \in \mathbb{N}. \tag{2}$$

The power flow models are also presented for maintaining the limitations of the voltage and current magnitudes of buses and lines as follows.

$$|V_n^{(min)}| \leq |V_n| \leq |V_n^{(max)}|; \quad \forall n \in \mathbb{N}, \tag{3}$$

$$0 \leq |I_{nn'}| \leq |I_{nn'}^{(max)}|; \quad \forall n, n' \in \mathbb{N}. \tag{4}$$

In the following, a number of power flow models are presented. Based on the requirements and the accuracy, each one of them can be adopted in the pre-scheduling (first-level) and on-line (second-level) optimization problems of the DiGriFlex project.

3.2.1.1. AC power flow

Each bus has an associated voltage phasor as well as active and reactive power injections. The voltage phasors are denoted by $\vec{V} \in \mathbb{C}^{|\mathbb{N}|}$, with polar coordinate representation $\overrightarrow{|V|} \angle \vec{\delta}$, where $\overrightarrow{|V|} > 0 \in \mathbb{R}^{|\mathbb{N}|}$ and $\vec{\delta} \in (-3.14, 3.14]^{|\mathbb{N}|}$.

The power flow equations are

$$P_n + jQ_n = V_n \sum_{n' \in \mathbb{N}} Y_{nn'}^* V_{n'}^*; \quad \forall n \in \mathbb{N}. \tag{5}$$

Splitting real and imaginary parts of (5) and using polar voltage coordinates yields

$$P_n = |V_n| \sum_{n' \in \mathbb{N}} |V_{n'}| \left(G_{nn'} cos(\delta_n - \delta_{n'}) + B_{nn'} sin(\delta_n - \delta_{n'}) \right); \quad \forall n \in \mathbb{N}, \tag{6}$$

$$Q_n = |V_n| \sum_{n' \in \mathbb{N}} |V_{n'}| \left(G_{nn'} sin(\delta_n - \delta_{n'}) - B_{nn'} cos(\delta_n - \delta_{n'}) \right); \quad \forall n \in \mathbb{N}. \tag{7}$$

In this power flow model, the current phasors of the lines are calculated as

$$I_{nn'} = Y_{nn'}(V_n - V_{n'}). \tag{8}$$

3.2.1.2. DistFlow model

The DistFlow model (9)-(12) fully represents the power flows for a balanced radial network. However, (9)-(12) is an approximation for meshed topologies power flows.

$$P_{nn'} = r_{nn'} l_{nn'} - P_{n'} + \sum_{n'' \in \Theta_{n'}} P_{n'n''}; \quad \forall n \in \mathbb{N}, \forall n' \in \Theta_n, \tag{9}$$

$$Q_{nn'} = x_{nn'} l_{nn'} - Q_{n'} + \sum_{n'' \in \Theta_{n'}} Q_{n'n''}; \quad \forall n \in \mathbb{N}, \forall n' \in \Theta_n, \tag{10}$$

$$v_n - v_{n'} = 2(r_{nn'} P_{nn'} + x_{nn'} Q_{nn'}) - (r_{nn'}^2 + x_{nn'}^2) l_{nn'}; \quad \forall n \in \mathbb{N}, \forall n' \in \Theta_n, \tag{11}$$

$$l_{nn'} v_n = P_{nn'}^2 + Q_{nn'}^2; \quad \forall n \in \mathbb{N}, \forall n' \in \Theta_n, \tag{12}$$

where each line has series impedance $r_{nn'} + j.x_{nn'}$.

In this power flow model, the current of lines are calculated as

$$I_{nn'} = \sqrt{l_{nn'}}. \tag{13}$$

To convexify the Distflow model, (12) can be replaced by the following inequality. The resulted power flow model can be solved with second-order cone programming (SOCP) solvers.

$$l_{nn'} v_n \geq P_{nn'}^2 + Q_{nn'}^2; \quad \forall n \in \mathbb{N}, \forall n' \in \Theta_n. \tag{14}$$

In [1], it is proved that this convex second-order relaxation is exact when the objective function of the problem is linear. For other problems, the exactness of this relaxation must be studied.

It is worth mentioning that in the DistFlow model it is implicitly assumed that the directions of active power through the lines are known. Set Θ_n is used here to denote the connected nodes that receive power from bus n. For the case of generation in dthe istribution grid, when the directions of active power are unknown, the DistFlow model is modified in [2] to compute the exact power flow. The following constraints are added into the model for considering the possibility of generation in the grid.

$$\hat{P}_{nn'}^{(T)} = -P_{n'} + \sum_{n'' \in \Theta_{n'}} \hat{P}_{n'n''}^{(T)}; \quad \forall n \in \mathbb{N}, \forall n' \in \Theta_n, \tag{15}$$

$$\hat{Q}_{nn'}^{(T)} = -Q_{n'} + \sum_{n'' \in \Theta_{n'}} \hat{Q}_{n'n''}^{(T)}; \quad \forall n \in \mathbb{N}, \forall n' \in \Theta_n, \tag{16}$$

$$\bar{v}_n - \bar{v}_{n'} = 2(r_{nn'} \hat{P}_{nn'}^{(T)} + x_{nn'} \hat{Q}_{nn'}^{(T)}); \quad \forall n \in \mathbb{N}, \forall n' \in \Theta_n, \tag{17}$$

$$\bar{P}_{nn'}^{(T)} = r_{nn'} \bar{l}_{nn'} - P_{n'} + \sum_{n'' \in \Theta_{n'}} \bar{P}_{n'n''}^{(T)}; \quad \forall n \in \mathbb{N}, \forall n' \in \Theta_n, \tag{18}$$

$$\bar{Q}_{nn'}^{(T)} = x_{nn'} \bar{l}_{nn'} - Q_{n'} + \sum_{n'' \in \Theta_{n'}} \bar{Q}_{n'n''}^{(T)}; \quad \forall n \in \mathbb{N}, \forall n' \in \Theta_n, \tag{19}$$

$$\bar{l}_{nn'} v_{n'} \geq max\{\hat{P}_{nn'}^{(B)}, \bar{P}_{nn'}^{(B)}\}^2 + max\{\hat{Q}_{nn'}^{(B)}, \bar{Q}_{nn'}^{(B)}\}^2; \quad \forall n \in \mathbb{N}, \forall n' \in \Theta_n, \tag{20}$$

$$\bar{l}_{nn'} v_n \geq max\{\hat{P}_{nn'}^{(T)}, \bar{P}_{nn'}^{(T)}\}^2 + max\{\hat{Q}_{nn'}^{(T)}, \bar{Q}_{nn'}^{(T)}\}^2; \quad \forall n \in \mathbb{N}, \forall n' \in \Theta_n, \tag{21}$$

$$\bar{P}_{nn'}^{(B)} = -P_{n'} + \sum_{n'' \in \Theta_{n'}} \bar{P}_{n'n''}^{(T)}; \quad \forall n \in \mathbb{N}, \forall n' \in \Theta_n, \tag{22}$$

$$\bar{Q}_{nn'}^{(B)} = -Q_{n'} + \sum_{n'' \in \Theta_{n'}} \bar{Q}_{n'n''}^{(T)}; \quad \forall n \in \mathbb{N}, \forall n' \in \Theta_n, \tag{23}$$

$$\hat{P}_{nn'}^{(B)} = -P_{n'} + \sum_{n'' \in \Theta_{n'}} \hat{P}_{n'n''}^{(T)}; \quad \forall n \in \mathbb{N}, \forall n' \in \Theta_n, \tag{24}$$

$$\hat{Q}_{nn'}^{(B)} = -Q_{n'} + \sum_{n'' \in \Theta_{n'}} \hat{Q}_{n'n''}^{(T)}; \quad \forall n \in \mathbb{N}, \forall n' \in \Theta_n, \tag{25}$$

$$|I_{nn'}^{(max)}| v_{n'} \geq max\{\hat{P}_{nn'}^{(B)}, \bar{P}_{nn'}^{(B)}\}^2 + max\{\hat{Q}_{nn'}^{(B)}, \bar{Q}_{nn'}^{(B)}\}^2; \quad \forall n \in \mathbb{N}, \forall n' \in \Theta_n, \tag{26}$$

$$|I_{nn'}^{(max)}| v_n \geq max\{\hat{P}_{nn'}^{(T)}, \bar{P}_{nn'}^{(T)}\}^2 + max\{\hat{Q}_{nn'}^{(T)}, \bar{Q}_{nn'}^{(T)}\}^2; \quad \forall n \in \mathbb{N}, \forall n' \in \Theta_n, \tag{27}$$

where $\hat{P}_{nn'}^{(T)}$, $\hat{Q}_{nn'}^{(T)}$, $\bar{P}_{nn'}^{(T)}$, $\bar{Q}_{nn'}^{(T)}$, $\hat{P}_{nn'}^{(B)}$, $\hat{Q}_{nn'}^{(B)}$, $\bar{P}_{nn'}^{(B)}$, $\bar{Q}_{nn'}^{(B)}$, $\bar{v}_n$, and $\bar{l}_{nn'}$ are auxiliary variables. In [2], it is discussed how adding these constraints may overcome the challenge of undefined directions of active power in distribution networks.

3.2.1.3. Linearized DistFlow model

By neglecting the losses in the DistFlow model (setting $l_{nn'} = 0$ to remove the terms related to the losses in (9)-(12)), the linearized Distflow model is derived as presented in the following. This new model can be included in a linear programming (LP) problem.

$$P_{nn'} = -P_{n'} + \sum_{n'' \in \Theta_{n'}} P_{n'n''}; \quad \forall n \in \mathbb{N}, \forall n' \in \Theta_n, \tag{28}$$

$$Q_{nn'} = -Q_{n'} + \sum_{n'' \in \Theta_{n'}} Q_{n'n''}; \quad \forall n \in \mathbb{N}, \forall n' \in \Theta_n, \tag{29}$$

$$v_n - v_{n'} = 2(r_{nn'} P_{nn'} + x_{nn'} Q_{nn'}); \quad \forall n \in \mathbb{N}, \forall n' \in \Theta_n. \tag{30}$$

In this power flow model, the current magnitudes of lines cannot be calculated directly. Thus, for the constraints related to current magnitudes (e.g., (4)), $|I_{nn'}|$ is overestimated as below:

$$|I_{nn'}| \approx \frac{max\{P_{nn'}, -P_{nn'}\} + max\{Q_{nn'}, -Q_{nn'}\}}{V_n^{min}}. \tag{31}$$

The maximum functions can be linearized easily using a number of inequalities.

3.2.1.4. Direct-Current (DC) power flow

The most commonly used linear approximation in the literature of power system is the DC power flow model, which is based on several assumptions.

- Reactive power flows can be neglected.
- The lines are lossless, i.e., $\vec{G} \approx 0$, and shunt elements can be neglected.
- The voltage magnitudes at all buses are approximately equal, so $|V_n| \approx 1 \text{ per unit}$ at all buses $n \in \mathbb{N}$.
- Angle differences between connected buses are small such that $sin(\delta_n - \delta_{n'}) \approx \delta_n - \delta_{n'}, \forall n \in \mathbb{N}, \forall n' \in \mathbb{N}'$.

Applying these assumptions, the following DC power flow model is derived:

$$\sum_{n' \in \Theta_n} B_{nn'}(\delta_n - \delta_{n'}) = P_n; \quad \forall n \in \mathbb{N}. \tag{32}$$

In this power flow model, the lines currents are calculated as follows.

$$I_{nn'} = B_{nn'}(\delta_n - \delta_{n'}). \tag{33}$$

Note that as the voltage magnitudes of nodes are not calculated in this model and the ratio of R/X is high in distribution grid. Thus, the DC power flow model is not an appropriate one for distribution grid modelling.

3.2.1.5. Convex DC power flow model

The flowing power through a line can be approximated as a convex function of the voltage angle differences. For derivation of convex DC approximation, we consider that $|V_n|$ is 1 per-unit for all buses. Moreover, the voltage angle differences, i.e., $\delta_n - \delta_{n'}$, are assumed enough small. By using this approximation, $sin(\delta_n - \delta_{n'})$ and $cos(\delta_n - \delta_{n'})$ can be approximated by $\delta_n - \delta_{n'}$ and $1 - 0.5(\delta_n - \delta_{n'})^2$, respectively.

Applying these assumptions, the following convex DC power flow model is derived:

$$P_n = \sum_{n' \in \Theta_n} [B_{nn'}(\delta_n - \delta_{n'}) + 0.5G_{nn'}(\delta_n - \delta_{n'})^2]; \quad \forall n \in \mathbb{N}. \tag{34}$$

In this power flow model, the lines currents are calculated as follows:

$$I_{nn'} = B_{nn'}(\delta_n - \delta_{n'}) + 0.5G_{nn'}(\delta_n - \delta_{n'})^2. \tag{35}$$

To construct a convex relaxation, both (34) and (35) can be replaced with the following inequalities. It can be proved that the same power flow is resulted considering the following inequalities instead of original equalities.

$$P_n \leq \sum_{n' \in \Theta_n} [B_{nn'}(\delta_n - \delta_{n'}) + 0.5G_{nn'}(\delta_n - \delta_{n'})^2]; \quad \forall n \in \mathbb{N}. \tag{36}$$

$$I_{nn'} \geq B_{nn'}(\delta_n - \delta_{n'}) + 0.5G_{nn'}(\delta_n - \delta_{n'})^2; \quad \forall n \in \mathbb{N}. \tag{37}$$

Same as DC power flow mode, the voltage magnitudes of nodes are not calculated in convex DC power flow model and the ratio of R/X is high in the distribution grid. Thus, the convex DC power flow model is not an appropriate model for the distribution grid modelling.

3.2.1.6. Linear power flow model

One approach for linearizing the power flow equations for distribution grids is based on linearization around the no-load voltage profile under the assumptions of negligible shunt impedances and near-optimal voltage magnitudes. The voltage magnitudes can then be approximated as functions of active and reactive power injection vectors $\vec{P}$ and $\vec{Q}$:

$$\overrightarrow{|V|} = 1 + \boldsymbol{R}\vec{P} + \boldsymbol{X}\vec{Q}, \tag{38}$$

where $\boldsymbol{Y}^{-1} := \boldsymbol{R} + j\boldsymbol{X}$.

The lines currents can also be approximated based on the no-load voltage profile and Jacobian matrix as described in [3].

3.2.1.7. Sensitivity-factor based model

The power flow equation can be written solely relying on the measurements, without using any information of the grid model. In the literature, the coefficients of sensitivity factors are defined for the voltage

magnitude sensitivities of node n or current magnitude of line from node n to node n' with respect to the injected active/reactive power of bus n'' as described in the following:

$$K_{nn''}^{(VP)} := \frac{\partial |V_n|}{\partial P_{n''}}, \quad K_{nn''}^{(VQ)} := \frac{\partial |V_n|}{\partial Q_{n''}}, \tag{39}$$

$$K_{nn'n''}^{(IP)} := \frac{\partial |I_{nn'}|}{\partial P_{n''}}, \quad K_{nn'n''}^{(IQ)} := \frac{\partial |I_{nn'}|}{\partial Q_{n''}}. \tag{40}$$

These sensitivity factors can be determined using data-driven approaches and relying solely on the measurements [4, 5]. Based on these sensitivity factors and assuming that the network operates around an operating point, the following equations can be derived.

$$|V_n| = |V_n^{(op)}| + \sum_{n'' \in \mathbb{N}} K_{nn''}^{(VP)} (P_{n''} - P_{n''}^{(op)}) + \sum_{n'' \in \mathbb{N}} K_{nn''}^{(VQ)} (Q_{n''} - Q_{n''}^{(op)}); \quad \forall n \in \mathbb{N}, \tag{41}$$

$$|I_{nn'}| = |I_{nn'}^{(op)}| + \sum_{n'' \in \mathbb{N}} K_{nn'n''}^{(IP)} (P_{n''} - P_{n''}^{(op)}) + \sum_{n'' \in \mathbb{N}} K_{nn'n''}^{(IQ)} (Q_{n''} - Q_{n''}^{(op)}); \quad \forall n \in \mathbb{N}, \tag{42}$$

here $|V_n^{(op)}|$, $|I_{nn'}^{(op)}|$, $P_n^{(op)}$, and $Q_n^{(op)}$ are the operating point of voltage magnitude, line current magnitude, active power, and reactive power, respectively.

3.2.1.8. Conclusion

The mentioned power flow models are summarized in Table 1.

For pre-scheduling (first-level) problem, the DistFlow (exact version in [2]) is adopted. The reason behind using this version is that the distribution grid is radial in most cases and in addition, there are generation and consumption in active distribution networks. Therefore, the directions of active power are unknown. For the on-line (second-level) problem, the sensitivity-factor based model is used if the exact DistFlow model generates a lot of variables and constraints. The reason behind using this model in the second-level problem is that the problem must be solved in a limited time. Therefore, a linear version of the constraints can be used, which leads us to a LP problem.

Table 1: The presented models of power flow.

Section	Name	Equations	Convex/Non-Convex	Meshed/Radial
5.1.1	AC	(5)-(8)	Non-Convex	Meshed
5.1.2	DistFlow	(9)-(11), (14), (15)-(27)	Non-Convex→SOCP	Radial
5.1.3	Linearized DistFlow	(28)-(31)	LP	Radial
5.1.4	DC	(32)-(33)	LP	Meshed
5.1.5	Convex DC	(36)-(37)	Non-Convex→SOCP	Meshed
5.1.6	Linear	(38)	LP	Meshed
5.1.7	Sensitivity-Factor Based	(39)-(42)	LP	Meshed

3.2.2 Constraints of battery energy storage systems (BESSs)

Several approaches exist for modelling the constraints of BESSs such as modelling the internal chemical state of charge (SOC) of the BESSs or modelling the BESSs as the equivalent electrical circuits. Here, the models based on internal chemical states of the BESSs are adopted. In the adopted models, the parameters of the BESSs can be obtained using the BESSs specification sheets.

Same as the models of power flow, the model of BESSs are given for a scenario in this section. The index of ω (referring to the scenario) is dropped here. Based on the requirements and necessities, this index must be added into the models.

3.2.2.1. Nonlinear model

Several real-world aspects of BESSs are incorporated in this model such as the limits on the SOC, maximum charging/discharging powers, and self-discharge. Nonlinear model is described using the following set of constraints:

$$\mathrm{SOC}_{s(t+1)} = (1-\gamma_s^{(LV)})\mathrm{SOC}_{st} + min\{\frac{P_{st}^{(BESS)}\Delta t}{\eta_s^{(D)}}, 0\} + max\{\eta_s^{(C)} P_{st}^{(BESS)}\Delta t, 0\} - \gamma_s^{(LC)}\Delta t; \quad \forall s \in \mathbb{S}, \forall t \in \mathbb{T}, \tag{43}$$

$$(P_{st}^{(BESS)})^2 + (Q_{st}^{(BESS)})^2 \leq (S_s^{(BESS,max)})^2; \quad \forall s \in \mathbb{S}, \forall t \in \mathbb{T}, \tag{44}$$

$$\mathrm{SOC}_s^{(min)} \leq \mathrm{SOC}_{st} \leq \mathrm{SOC}_s^{(max)}; \quad \forall s \in \mathbb{S}, \forall t \in \mathbb{T}. \tag{45}$$

It is worth mentioning that this model does not reflect the well-known physical phenomenon that the BESSs capacities change with applying different charging/discharging currents. This behavior is observed specifically in Li-ion batteries. In addition, it is assumed that both the charging/discharging efficiencies of the BESSs are constants; whereas in reality they depend on the magnitude of the charging current.

3.2.2.2. Mixed-integer linear programming (MILP) model

The presented first model is non-convex due to the presence of $\min\{.\}$ and $\max\{.\}$ functions in (43). To solve an optimization problem including these constraints with a commercial solver, a MILP model can be used by defining auxiliary variables $P_{st}^{(BESS,D)}$, $P_{st}^{(BESS,C)}$, and binary variables $u_{st}^{(BESS,D)}$, $u_{st}^{(BESS,C)}$, and rewriting (43) as below.

$$\mathrm{SOC}_{s(t+1)} = (1-\gamma_s^{(LV)})\mathrm{SOC}_{st} + \frac{P_{st}^{(BESS,D)}\Delta t}{\eta_s^{(D)}} + \eta_s^{(C)} P_{st}^{(BESS,C)}\Delta t - \gamma_s^{(LC)}\Delta t; \forall s \in \mathbb{S}, \forall t \in \mathbb{T}, \tag{46}$$

$$0 \leq P_{st}^{(BESS,C)} \leq S_s^{(BESS,max)} u_{st}^{(BESS,C)}; \quad \forall s \in \mathbb{S}, \forall t \in \mathbb{T}, \tag{47}$$

$$-S_s^{(BESS,max)} u_{st}^{(BESS,D)} \leq P_{st}^{(BESS,D)} \leq 0; \quad \forall s \in \mathbb{S}, \forall t \in \mathbb{T}, \tag{48}$$

$$u_{st}^{(BESS,D)} + u_{st}^{(BESS,D)} \leq 1; \quad \forall s \in \mathbb{S}, \forall t \in \mathbb{T}, \tag{49}$$

$$u_{st}^{(BESS,D)}, u_{st}^{(BESS,D)} \in \{0,1\}; \quad \forall s \in \mathbb{S}, \forall t \in \mathbb{T}, \tag{50}$$

$$P_{st}^{(BESS)} = P_{st}^{(BESS,C)} - P_{st}^{(BESS,D)}; \quad \forall s \in \mathbb{S}, \forall t \in \mathbb{T}, \tag{51}$$

$$\mathrm{SOC}_s^{(min)} \leq \mathrm{SOC}_{st} \leq \mathrm{SOC}_s^{(max)}; \quad \forall s \in \mathbb{S}, \forall t \in \mathbb{T}. \tag{52}$$

In this version of the model, the reactive power injection of BESS is forced to be zero. If we consider the reactive power injection of BESS to be non-zero, the constraints fit into mixed-integer second order cone programming (MISOCP) problems.

3.2.2.3. Convex model

Solving the MILP problems has high computational complexity. We can use the following method to turn the non-convex constraints of BESSs into the convex ones.

The integer variables in (47)-(48) are introduced because of the differences between magnitudes of efficiencies $\eta_s^{(D)}$ and $\eta_s^{(C)}$. In addition, to force the BESSs to work in one operating mode (charging or discharging) at each single time step. As formulated in [6], we can remove these binary variables and it is not necessary to have them since giving values to both charging and discharging power variables results in increased energy losses and, consequently, increases the objective function. However, removing these binary variables could be misused to create an unreal load to satisfy security constraints in the presence of large amount of injections into the grid. In this respect, we have added an auxiliary SOC variable, i.e., $\widetilde{\mathrm{SOC}}_{s(t+1)}$, and its respective constraint, assuming an ideal BESS efficiency. This auxiliary constraint is necessary to avoid the ill use of the relaxed BESS efficiencies in order to create an unreal load. This modified convex model of (46)-(52) is presented in the following.

$$\mathrm{SOC}_{s(t+1)} = (1-\gamma_s^{(LV)})\mathrm{SOC}_{st} + \frac{P_{st}^{(BESS,D)}\Delta t}{\eta_s^{(D)}} + \eta_s^{(C)} P_{st}^{(BESS,C)}\Delta t - \gamma_s^{(LC)}\Delta t; \quad \forall s \in \mathbb{S}, \forall t \in \mathbb{T}, \tag{53}$$

$$0 \le P_{st}^{(BESS,C)} \le S_s^{(BESS,max)}; \quad \forall s \in \mathbb{S}, \forall t \in \mathbb{T}, \tag{54}$$

$$-S_s^{(BESS,max)} \le P_{st}^{(BESS,D)} \le 0; \quad \forall s \in \mathbb{S}, \forall t \in \mathbb{T}, \tag{55}$$

$$P_{st}^{(BESS)} = P_{st}^{(BESS,C)} - P_{st}^{(BESS,D)}; \quad \forall s \in \mathbb{S}, \forall t \in \mathbb{T}, \tag{56}$$

$$(P_{st}^{(BESS)})^2 + (Q_{st}^{(BESS)})^2 \le (S_s^{(BESS,max)})^2; \quad \forall s \in \mathbb{S}, \forall t \in \mathbb{T}, \tag{57}$$

$$\mathrm{SOC}_s^{(min)} \le \mathrm{SOC}_{st} \le \mathrm{SOC}_s^{(max)}; \quad \forall s \in \mathbb{S}, \forall t \in \mathbb{T}, \tag{58}$$

$$\widetilde{\mathrm{SOC}}_{s(t+1)} = (1-\gamma_s^{(LV)})\widetilde{\mathrm{SOC}}_{st} + P_{st}^{(BESS,D)}\Delta t + P_{st}^{(BESS,C)}\Delta t - \gamma_s^{(LC)}\Delta t; \quad \forall s \in \mathbb{S}, \forall t \in \mathbb{T}, \tag{59}$$

$$\mathrm{SOC}_s^{(min)} \le \widetilde{\mathrm{SOC}}_{st} \le \mathrm{SOC}_s^{(max)}; \quad \forall s \in \mathbb{S}, \forall t \in \mathbb{T}. \tag{60}$$

In this model, the reactive power injection of BESSs, i.e., $Q_{st}^{(BESS)}$, are considered and can have non-zero values. The model also remains convex and suitable for SOCP problems.

3.2.2.4. Conclusion

The mentioned models for BESSs are summarized in Table 2.

For the pre-scheduling (first-level) problem, the convex model (the relaxed model described in [6]) is used. For the on-line (second-level) problem, we need a linear model. The only nonlinear constraint exists in the model (53)-(60) is constraint (57). To linearize this constraint, we can use the approach of [7]. We approximate a circle with radius of $S_s^{(BESS,max)}$ with a couple of linear lines.

Table 2: The presented models of BESSs.

Section	Name	Equations	Convex/Non-Convex	Reactive power
5.2.1	Nonlinear	(43)-(45)	Non-Convex	Considered
5.2.2	MILP	(45)-(52)	MILP	Neglected
5.2.3	Convex	(53)-(60)	Convex→SOCP	Considered

3.2.3 Constraints of PVs

The capability curve of a PV system is defined with the following limitations, which are illustrated in Figure 5:

- The converter voltage limit,
- The converter current limit,
- Maximum power because of available solar irradiance.

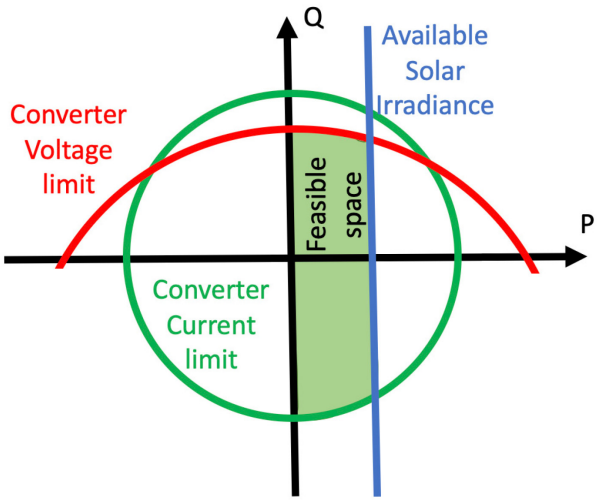

Figure 5: The capability constraints of PVs [8].

These constraints are normally convex; however, we can develop a linear version of these constraints. In the following, both versions of convex and linear formats are presented.

Here, both models are given for one time step and a single scenario. The indices of t and ω (referring to the time-step and scenario, respectively) are dropped here. Based on the requirements and necessities, these indices must be added in the models.

3.2.3.1. Convex model

As it is proved in [8], the converter voltage limit of a PV system can be written as a circle with a centre of $-3(V_i^{(grid,PV)})^2/X_i^{(PV)}$ in the Q-axis and a radius of $3V_i^{(grid,PV)}V_i^{(conv,PV)}/X_i^{(PV)}$.

$$(P_i^{(PV)})^2 + (Q_i^{(PV)} + \frac{3(V_i^{(grid,PV)})^2}{X_i^{(PV)}})^2 \leq (\frac{3V_i^{(grid,PV)}V_i^{(conv,PV)}}{X_i^{(PV)}})^2; \quad \forall i \in \mathbb{I}, \tag{61}$$

here, $V_i^{(grid,PV)}$, $V_i^{(conv,PV)}$, and $X_i^{(PV)}$ are grid voltage, converter voltage, and Thevenin reactance from the viewpoint of PV production system i, repsectively.

The converter current limit of a PV production system can be presented by a circle with radius of $S_i^{(PV,max)}$ as follows:

$$(P_i^{(PV)})^2 + (Q_i^{(PV)})^2 \leq (S_i^{(PV,max)})^2; \quad \forall i \in \mathbb{I}. \tag{62}$$

Finally, the available solar irradiance and positive generation limits are presented with the following constraints:

$$0 \leq P_i^{(PV)} \leq P_i^{(PV,max)}; \quad \forall i \in \mathbb{I}. \tag{63}$$

3.2.3.2. Linear model

The power capability of a PV system can be linearized using a predefined number of linear boundaries. For instance, instead of (61) and (61), the following two linear constraints are considered.

$$K_i^{(PV1)} P_i^{(PV)} + Q_i^{(PV)} \leq K_i^{(PV2)}; \quad \forall i \in \mathbb{I}, \tag{64}$$

$$K_i^{(PV3)} P_i^{(PV)} + Q_i^{(PV)} \leq K_i^{(PV4)}; \quad \forall i \in \mathbb{I}, \tag{65}$$

in which,

$$K_i^{(PV1)} = \left(\frac{3V_i^{(grid,PV)} V_i^{(conv,PV)}}{X_i^{(PV)}} - \sqrt{(\frac{3(V_i^{(grid,PV)})^2}{X_i^{(PV)}})^2 - (P_i^{(PV,max)})^2} \right) \frac{1}{P_i^{(PV,max)}}, \tag{66}$$

$$K_i^{(PV2)} = \frac{3V_i^{(grid,PV)} V_i^{(conv,PV)} - 3(V_i^{(grid,PV)})^2}{X_i^{(PV)}}, \tag{67}$$

$$K_i^{(PV3)} = \left(S_i^{(PV,max)} - \sqrt{(S_i^{(PV,max)})^2 - (P_i^{(PV,max)})^2} \right) \frac{1}{P_i^{(PV,max)}}, \tag{68}$$

$$K_i^{(PV4)} = S_i^{(PV,max)}. \tag{69}$$

Therefore, the linear model of PV system constraints includes (63)-(69).

3.2.3.3. Conclusion

The mentioned models for the PV systems are summarized in the Table 3. For the pre-scheduling (first-level) problem, the convex model is used. For the on-line (second-level) problem, the linear model is adopted.

Table 3: The presented models of PV systems.

Section	Name	Equations	Convex/Non-Convex
5.3.1	Convex	(61)-(63)	Convex
5.3.2	Linear	(63)-(69)	LP

3.2.4 Constraints of connection points

The distribution grids can have multiple connecting nodes to the upper layer grids, in which these nodes are denoted by index $n \in \mathbb{N}^{(TC)}$. These nodes are considered as slack nodes in both of pre-scheduling and on-line problems. In the power flow model (Distflow and Sensitivity factor based models), we do not have phase angle variables; thus, the voltage magnitude of these slack nodes should be known as parameters. However, the voltage magnitudes of these nodes depend on the neighbouring distribution networks power flow that are not modelled in this study. As a result, the voltage magnitudes of slack

nodes are considered as uncertain parameters that we do not have any information from the probability distributions of them. We only know the boundaries of these uncertain parameters.

In the proposed scheduling problem, we want to find the active and reactive power injections of these nodes that are offered to the day-ahead market. They are denoted by $P_{nt}^{(SC)}$ and $Q_{nt}^{(SC)}$. In addition, we want to find the active and reactive power reserves (for both upward and downward movements), which are denoted by $R_{nt}^{(SC,f)}: f \in \{P+, P-, Q+, Q-\}$.

In each scenario of operation, i.e., $\omega \in \Omega$, the upper layer grid operator may ask from the distribution system operator (DSO) to provide the reserves equal to $r_{nt\omega}^{(RT,P)}$ and $r_{nt\omega}^{(RT,Q)}$. These values of deployed reserves must be within the boundaries of what DSO offered, i.e., $-R_{nt}^{(SC,P-)} \leq r_{nt\omega}^{(RT,P)} \leq R_{nt}^{(SC,P+)}$ and $-R_{nt}^{(SC,Q-)} \leq r_{nt\omega}^{(RT,Q)} \leq R_{nt}^{(SC,Q+)}$.

If the DSO cannot provide these flexibilities and instead provides the active and reactive power equal to $P_{nt\omega}^{(RT)}$ and $Q_{nt\omega}^{(RT)}$, the deviations are as follows.

$$\alpha_{nt\omega}^{(P+)} = max\{ P_{nt\omega}^{(RT)} - P_{nt}^{(SC)} - r_{nt\omega}^{(RT,P)}, 0\}; \quad \forall n \in \mathbb{N}^{(TC)}, \forall t \in \mathbb{T}, \forall \omega \in \Omega, \tag{70}$$

$$\alpha_{nt\omega}^{(P-)} = -min\{ P_{nt\omega}^{(RT)} - P_{nt}^{(SC)} - r_{nt\omega}^{(RT,P)}, 0\}; \quad \forall n \in \mathbb{N}^{(TC)}, \forall t \in \mathbb{T}, \forall \omega \in \Omega, \tag{71}$$

$$\alpha_{nt\omega}^{(Q+)} = max\{ Q_{nt\omega}^{(RT)} - Q_{nt}^{(SC)} - r_{nt\omega}^{(RT,Q)}, 0\}; \quad \forall n \in \mathbb{N}^{(TC)}, \forall t \in \mathbb{T}, \forall \omega \in \Omega, \tag{72}$$

$$\alpha_{nt\omega}^{(Q-)} = -min\{ Q_{nt\omega}^{(RT)} - Q_{nt}^{(SC)} - r_{nt\omega}^{(RT,Q)}, 0\}; \quad \forall n \in \mathbb{N}^{(TC)}, \forall t \in \mathbb{T}, \forall \omega \in \Omega. \tag{73}$$

Note that the constraints (70)-(73) can be linearized using auxiliary variables. In addition, all these constraints can be used for both pre-scheduling and on-line optimization problems in the next section. The slight difference would be for on-line optimization problem, $P_{nt}^{(SC)}$ and $Q_{nt}^{(SC)}$ are parameters while they are variables in the pre-scheduling optimization problem and they should be determined as outputs of the problem.

3.3 Choice and setup of mathematical formulation

In this section, the mathematical formulations, including the objective and constraints for both pre-scheduling (first-level) and on-line (second-level) problems are given. To find an appropriate model for pre-scheduling problem complying with the uncertainty in accordance with the outcomes of WP2, two models of stochastic programming and distributionally robust optimization are presented. The solution approaches of these two models are compared and the best one is chosen according to the nature of the problem. Finally, the setup of the pre-scheduling problem interface with on-line problem is introduced.

3.3.1 Pre-scheduling (first-level) optimization problem

The inputs of this optimization problem are introduced before. Here, we are writing a problem to find a robust solution against the uncertain parameters $|V_{nt\omega}|: n \in \mathbb{N}^{(TC)}$, $P_{dt\omega}^{(DEM)}$, $Q_{dt\omega}^{(DEM)}$, $P_{it\omega}^{(PV,max)}$, $r_{nt\omega}^{(RT,P)}$, and $r_{nt\omega}^{(RT,Q)}$. Finding the probability distribution functions for some of these uncertain parameters (such as $P_{dt\omega}^{(DEM)}$, $Q_{dt\omega}^{(DEM)}$, $P_{it\omega}^{(PV,max)}$,) is possible. However, forecasting the uncertain parameters $|V_{nt\omega}|: n \in \mathbb{N}^{(TC)}$, $r_{nt\omega}^{(RT,P)}$, and $r_{nt\omega}^{(RT,Q)}$ is not possible and the boundaries of these uncertain parameters are just observable.

In the following, the pre-scheduling (first-level) problem is written using stochastic programming and distributionally robust programming. The advantages/disadvantages of adopting these two methods are discussed/compared.

3.3.1.1. Stochastic programming and its solution approach

In this version of scheduling optimization problem, a number of scenarios $\omega \in \Omega$ is generated and a stochastic programming problem is written. The following stochastic optimization problem is solved in the day-ahead time scale to find the schedules of PVs and BESSs. In addition, by solving this problem, the energy, $P_{nt}^{(SC)}$ and $Q_{nt}^{(SC)}$, and reserves offers, $R_{nt}^{(SC,f)}: f \in \{P+, P-, Q+, Q-\}$, of DSO to the day-ahead market are determined.

$$min_{\Xi^{(SC)}} \sum_{t\in\mathbb{T}} \sum_{n\in\mathbb{N}^{(TC)}} \left(\lambda_{nt}^{(P)}.P_{nt}^{(SC)} + \lambda_{nt}^{(Q)}.Q_{nt}^{(SC)} - \sum_{f\in\{P+,P-,Q+,Q-\}} \lambda_{nt}^{(f)}.R_{nt}^{(SC,f)} \right) + \sum_{t\in\mathbb{T}} \mathbb{E}_{\omega} \left[\min_{\Xi_{t\omega}^{(RT)}:\forall\omega\in\Omega} \sum_{n\in\mathbb{N}^{(TC)}} \sum_{f\in\{P+,P-,Q+,Q-\}} BigM.\alpha_{nt\omega}^{(f)} \right] \quad (74)$$

Subject to:

Basic constraints: (1)-(4) and (70)-(73); $\forall t \in \mathbb{T}, \forall \omega \in \Omega$, (75)

Power flow (exact DistFlow model): (9)-(27);$\forall \omega \in \Omega$, (76)

Convex model of BESSs: (53)-(60);$\forall t \in \mathbb{T}, \forall \omega \in \Omega$, (77)

Convex model of capability constraints of PVs: (61)-(63);$\forall t \in \mathbb{T}, \forall \omega \in \Omega$, (78)

Here, the first line of the objective function is the costs of purchased active and reactive power from the upper layer grid minus the income of sold flexibility services. The cost of purchased active/reactive power is multiplication of the price, i.e., $\lambda_{nt}^{(P)}$ and $\lambda_{nt}^{(Q)}$, and the amount of scheduled active/reactive power, i.e., $P_{nt}^{(SC)}$ and $Q_{nt}^{(SC)}$. The income of sold flexibility service $f \in \{P+, P-, Q+, Q-\}$ is also computed by multiplying its price, i.e., $\lambda_{nt}^{(f)}$, and its scheduled capacity $R_{nt}^{(SC,f)}$. The flexibility services prices and energy price are determined in the WP 1 of this project. Here, in the objective (74), the second line is added to minimize the deviation from the upper layer system operator commands. This deviation is our last resource to make the problem feasible; thus, we use the large constant $BigM$ to be multiplied by the deviation $\alpha_{nt\omega}^{(f)}$ to penalize the objective in the case of using this last resource. It is worth mentioning that the deviation $\alpha_{nt\omega}^{(f)}$ is written for all scenario ω and the expectation over ω is established in the objective function.

The proposed stochastic problem is a two-stage (min-min) problem. Set $\Xi^{(SC)}$ includes the variables of upper level problem and the set $\Xi_{\omega}^{(RT)}$ consists of the variables of lower level for each scenario of operation. Set $\Xi^{(SC)}$ includes the following variables:

- $P_{nt}^{(SC)}$ and $Q_{nt}^{(SC)}$.
- $R_{nt}^{(SC,f)}: \forall f \in \{P+, P-, Q+, Q-\}$.

Set $\Xi_{\omega}^{(RT)}$ includes the following variables:

- $P_{it\omega}^{(PV)}$ and $Q_{it\omega}^{(PV)}$.
- $\mathrm{SOC}_{st\omega}$, $P_{st\omega}^{(BESS)}$, and $Q_{st\omega}^{(BESS)}$.
- $v_{nt\omega}$ and $l_{nn't\omega}$, and all variables related to the exact Distflow model in (9)-(27).
- $P_{nt\omega}^{(RT)}$ and $Q_{nt\omega}^{(RT)}$.

In the following, we discuss the solution approach of this stochastic programming.

This min-min problem can be transformed into a single level problem as variables in the set $\Xi^{SC} \cup (\cup_{\omega\in\Omega} \Xi_{\omega}^{RT})$ can be determined simultaneously. By adopting the models of power flow, BESSs, and capability constraints of PVs, the proposed single-level stochastic optimization problem is solvable using SOCP, which has the desired accuracy and computational burden.

There are three methods to determine the scenarios of operation in stochastic programming: (i) Using probability distribution functions of uncertain parameters and finding representative scenarios, (ii) Vertex enumeration, and (iii) Selecting vertices randomly.

(i) In the first method, a high number of scenarios is generated using the probability distribution functions of uncertain parameters. For maximum production of PVs and demands consumptions, the forecasting system, proposed in the WP 2 of this project, gives us their probability distribution functions using historical data. However, for uncertain parameters $|V_{nt\omega}|: n \in \mathbb{N}^{(TC)}$, $r_{nt\omega}^{(RT,P)}$, and $r_{nt\omega}^{(RT,Q)}$, finding the probability distribution functions is not possible since the behaviors of these parameters do not depend on the historical data or there are not enough historical data for forecasting. To solve this issue, we can consider the worst case and boundaries of these variables. In other words, the boundary values (maximum and minimum permissible magnitudes of $|V_{nt\omega}|: n \in \mathbb{N}^{(TC)}$, $r_{nt\omega}^{(RT,P)}$, and $r_{nt\omega}^{(RT,Q)}$) are used and the uniform probability distribution function is considered within these boundary values.

To satisfy an ϵ -level of feasible solution (when constraints are satisfied for more than $(1-\epsilon)*100\%$ of realization of scenarios), and for the confidence-level $0 \leq \beta \leq 1$, the number of scenarios N must be selected according to the following rule [9].

$$\sum_{k=0}^{n_x-1} \binom{N}{k} \epsilon^k (1-\epsilon)^{N-k} \leq \beta, \tag{79}$$

where, n_x is the number of variables of stochastic optimization problem. By using this formula, the number of required scenario to ensure the ϵ -level of feasibility would be enormous for our proposed formulation and the problem becomes intractable.

(ii) In the second method of scenario generation, we only focus on the boundaries of uncertain parameters. In this method, we do not need the probability distribution functions of uncertain parameters. Problems whose constraint functions are linear, monotone, or convex (and the proposed scheduling problem is convex), it suffices to enforce the constraints only for the uncertainty vectors that correspond to the vertices/boundaries. Following this vertex enumeration scheme results in total with 2^{n_δ} scenarios [9]. Here, n_δ is the number of uncertain parameters. For the cases that the vertex enumeration approach leads us to a computationally manageable problem, no additional structure on the objective function and the constraints of the initial problem is required. However, in this proposed stochastic optimization problem, the number of scenarios becomes too high and using this method is impossible.

(iii) In the third method, we select a finite predetermined number of scenarios randomly from the vertices of uncertain parameters. Unlike the first method, we focus on the vertices in the third method. Unlike the second method, all the vertices are not enumerated. Since the proposed pre-scheduling problem is convex, it suffices to enforce the constraints only for vertices and we know that in the worst case, we should generate number of scenarios N according to (79). It is expected that the required number of scenarios should be less than the one determined from (79). However, there is not any mathematical proof for this statement and the number of scenarios depends on the problem parameters. Therefore, the challenge of required computation time for solving the stochastic programming version of the pre-scheduling optimization problem is remained while the only feasible and less time-consuming method for scenario generation for this stochastic optimization problem is the third method. We use this third method for comparing the proposed stochastic programming with another approach for modeling the pre-scheduling problem.

3.3.1.2. Distributionally robust programming and its solution approach

To solve the issues of stochastic programming [10], this new approach of distributionally robust programming is introduced in this section. This approach unlike the robust programming does not find the worst-case scenario in the objective function. Each scenario of forecast is considered as the sum of expectation of forecast and the deviation error around that expected value. In the proposed distributionally robust programming, we linearize all variables and power flow equations around the expectation of forecast value.

For implementing this model, we need to introduce the affinely distributionally robust counterpart constraints, introduced in the Appendix A. The main added constraint is the following chance constraint, in which it is added for limiting the deviation of active/reactive power of connection points with respect to the commands of upper layer grid system operator.

$$Prob\left(\sum_{n\in\mathbb{N}^{(TC)}} \alpha_{nt}^{(f)} \le \delta\right) \le 1-e; \forall t \in \mathbb{T}, \forall f \in \{P+, P-, Q+, Q-\}, \tag{80}$$

where, δ is a small constant and $1-e$ is the confidence-level.

Then, the distributionally robust optimization problem becomes as below:

$$min_{\Xi^{(SC)}} \sum_{t\in\mathbb{T}} \sum_{n\in\mathbb{N}^{(TC)}} \left(\lambda_{nt}^{(P)}.P_{nt}^{(SC)} + \lambda_{nt}^{(Q)}.Q_{nt}^{(SC)} - \sum_{f\in\{P+,P-,Q+,Q-\}} \lambda_{nt}^{(f)}.R_{nt}^{(SC,f)} \right) \tag{81}$$

Subject to:

Basic constraints: (1)-(4) and (70)-(73); $\forall t \in \mathbb{T}, \forall \omega \in \{0\}$, (82)

Power flow (exact DistFlow model): (9)-(27);$\forall \omega \in \{0\}$, (83)

Convex model of BESSs: (53)-(60);$\forall t \in \mathbb{T}, \forall \omega \in \{0\}$, (84)

Convex model of capability constraints of PVs: (61)-(63);$\forall t \in \mathbb{T}, \forall \omega \in \{0\}$, (85)

Affinely distributionally robust counterpart constraints: (80), (92)-(132);$\forall t \in \mathbb{T}$, (86)

here, the set of decision variables $\Xi^{(SC)}$ also includes the participation factors $\alpha_{it}^{(PV,P+)}$, $\alpha_{it}^{(PV,P-)}$, $\alpha_{it}^{(PV,Q+)}$, $\alpha_{it}^{(PV,Q-)}$, $\alpha_{st}^{(BESS,P+)}$, $\alpha_{st}^{(BESS,P-)}$, $\alpha_{st}^{(BESS,Q+)}$, $\alpha_{st}^{(BESS,Q-)}$, $\alpha_{nt}^{(RT,P+)}$, $\alpha_{nt}^{(RT,P-)}$, $\alpha_{nt}^{(RT,Q+)}$, and $\alpha_{nt}^{(RT,Q-)}$ to compensate the uncertainties.

In the following, we discuss the solution approach of this stochastic programming.

This new problem is written here only for one scenario $\omega = 0$ and the index of ω for all variables can be dropped. Therefore, the dimension of the problem becomes manageable. The only nonlinear constraint is (80) that makes the problem nonlinear. The Chebyshev inequality theorem (see [11]) is used to convexify the chance constraint. The assumption behind using Chebyshev inequality theorem is that uncertain variables have Gaussian probability distribution and each one of them is within mentioned boundaries with a specific confidence (these confidence-levels are denoted by $\theta_n^{(V)}$, $\theta_d^{(P,DEM)}$, $\theta_d^{(Q,DEM)}$, $\theta_i^{(PV)}$, $\theta_n^{(RT,P)}$, and $\theta_n^{(RT,Q)}$).

It is worth mentioning that in Appendix B, it is explained how to use the Chebyshev inequality theorem for replacing the constraint (80) with a linearized one.

3.3.1.3. Choosing appropriate model for pre-scheduling problem

The advantages of using distributionally robust programming instead of stochastic programming for pre-scheduling problem are as follow:

- The distributionally robust programming is written for the main forecasted scenario and it needs less computational burden compared to the stochastic programming.
- For generating the representative scenarios, which is used in stochastic programming, we need big historical data that is not available most of the times in LV distribution grids. Whereas the distributionally robust programming does not require this big historical data since it needs only the boundaries of uncertain variables.
- For LV distribution grids with many control/state variables, solving the stochastic programming with high number of scenarios is not achievable.

Because of above mentioned advantages of distributionally robust programming, it is more proper to use it in the pre-scheduling (first-level) problem. The performance of these two models are compared in a case study with numerical validation.

3.3.2 On-line (second-level) optimization problem

In on-line (second-level) optimization problem, the forecasting is updated and a deterministic forecast is derived (as one of the outputs of WP 2 of this project). Then, we have one scenario for each uncertain parameter. The set of decision variables of the on-line optimization problem, i.e., set $\Xi^{(RT)}$, includes the following control and state variables.

- $P_i^{(PV)}$ and $Q_i^{(PV)}$.
- SOC_s, $P_s^{(BESS)}$, and $Q_s^{(BESS)}$.
- v_n and $l_{nn'}$, and all variables related to the exact Distflow model in (9)-(27).
- $P_n^{(RT)}$ and $Q_n^{(RT)}$.

The on-line optimization problem should be solved within the duration of a time step as the solution must be available before the start of of next time step. In this study, the time step in real-time is considered equal to 10 minutes as the measurements in the distribution grid are available every 10 minutes. Since the forecasting algorithm is in series with the main optimization problem from the viewpoint of execution, the required time for forecasting algorithm should be considered and the sum of both forecasting algorithm and proposed real-time optimization problem should be less than 10 minutes. To this end, the main problem is written for only the forecasted scenario to find the solution in a limited time.

Note that the market prices of active/reactive power are available every 15 minutes in the national grid scale; however, the on-line optimization problem finds the dispatch for minimizing the deviation from the scheduled values. In addition, the real-time prices of active/reactive power are not considered in this project.

The following optimization problem is written to decide the schedule of PV production systems and BESSs in real-time.

$$min_{\Xi^{(RT)}} \sum_{n\in\mathbb{N}^{(TC)}} \sum_{f\in\{P+,P-,Q+,Q-\}} fac_1.\alpha_{nt\omega}^{(f)} + \sum_{s\in\mathbb{S}} fac_2.\left|\mathrm{SOC}_s - \widetilde{\mathrm{SOC}}_s\right| + \sum_{n\in\mathbb{N}}\sum_{n'\in\mathbb{N}} fac_3.R_{nn'}.|I_{nn'}|^2 \quad (87)$$

Subject to:

Basic constraints: (1)-(4) and (70)-(73); $\forall t \in \mathbb{T}, \forall \omega \in \{0\}$, (88)

Power flow (exact DistFlow model): (9)-(27);$\forall \omega \in \{0\}$, (89)

Convex model of BESSs: (53)-(60);$\forall t \in \mathbb{T}, \forall \omega \in \{0\}$, (90)

Convex model of capability constraints of PVs: (61)-(63);$\forall t \in \mathbb{T}, \forall \omega \in \{0\}$, (91)

where, $\widetilde{\mathrm{SOC}}_s$ is the schedule of BESS s, and the factors fac_1, fac_2, and fac_3 determine the priorities of minimization of deviation from the commands of upper layer grid system operator, deviation from the schedule of BESSs, and loss. In practice, these factors are selected such that $fac_1 > fac_2 > fac_3$; thus, minimizing the deviation from the commands of upper layer grid system operator has the highest priority. Then, minimizing the deviation from the schedule of BESSs, determined in the pre-scheduling problem, has higher priority compared to the loss minimization.

3.3.3 Interface of pre-scheduling and on-line optimization problems

After solving the pre-scheduling optimization problem, the interfaces between pre-scheduling and on-line optimization problems are:

- active and reactive power offers to the day-ahead market at the connection nodes ($P_{nt}^{(SC)}$ and $Q_{nt}^{(SC)}$),
- active and reactive power flexibility services offered to the day-ahead market at the connection nodes ($R_{nt}^{(SC,f)}$: $\forall f \in \{P+, P-, Q+, Q-\}$), and
- schedules of BESSs (SOC_{st0}).

As one can see, the result of on-line (second-level) problem depends on these interface variables.

To test the performance of pre-scheduling and on-line optimization problems, using Monte-Carlo simulation, a number of out-of-sample scenarios is generated. After finding the results of pre-scheduling optimization, we will run the on-line optimization for these out-of-sample scenarios.

It is worth mentioning that the pre-scheduling problem can be solved using stochastic programming based on a number of in-sample scenarios, which are different from these out-of-sample scenarios. By observing the performance of the results of prescheduling problem in these out-of-sample scenarios, we can get feedback from the on-line optimization (as it is promised in Figure 2). This feedback is in the terms of the income of distribution grid by participation in the energy market and deviation from the scheduled values. Then, the results of pre-scheduling problem can be updated considering this feedback. For updating the results of pre-scheduling problem, the confidence-level $1 - e$ of distributionally robust programming can be updated to have more conservative or more profitable solution.

4 Markov Chains based model

A randomized sampling approach based on historical data or knowledge of the probability density functions of the uncertain parameters is required for the proposed stochastic optimization problem. In order to accomplish this,
We created a data-driven scenario selection strategy based on the Markov chains. It is important to note that the solution to the stochastic optimization problem is robust if the number of scenarios, i.e., K, is large enough. Based on the results of [15], the minimum number of scenarios for establishing different confidence levels can be determined. However, the number of scenarios in the typical cases of our problem is so large that the resulting problem is not scalable. The required number of scenarios for our case study is more than 10000, where the ADN has just 5 buses and the problem is formulated for 144 time-steps (24 x 6 of 10 minutes time-steps). As a result, we assume a fixed and small number of representative scenarios based on historical data. In the sense that they exhibit the same behavior as a large number of scenarios, these scenarios are efficient.

The following is an explanation of the proposed method:

- Data preprocessing: We arrange the data of solar irradiance and electricity demand from the previous month. The data are then normalized by removing outliers and standardizing it based on minimum and maximum values. The data are then clustered into specific numbers, such as 3 clusters representing cloudy, intermittent cloudy, or clear days, using the K-Means method. This feature, known as cluster number, is added.
- Train the model: For each cluster number, we train a model based on Markov chain. As a result, we have matrices of transition probabilities for each cluster number.
- Forecasting: To forecast the uncertain parameters for the next day, we apply the model Random Forest. The resulting forecast is referred to as the baseline scenario.
- Scenario generation: We determine which cluster number is associated with the baseline scenario using the distance between the forecast and cluster centers. Then, using the associated transition matrix, we generate a large number of scenarios for that cluster number.
- Scenario reduction: We use the K-Means method to group the generated scenarios into a small number. Cluster centers are regarded as representative scenarios in addition to the baseline scenario previously forecasted.

4.1 Benchmark Scenario Selection Strategies

In order to quantify the merits of our proposed scenario selection strategy (which is presented in the next subsection), we look at two benchmark scenario selection strategies.

The first benchmark strategy is based on last month's data for an uncertain parameter, which is clustered into a small number. We use the method K-Means to cluster the data from the previous month, and the centers of clusters are regarded as scenarios. The drawback of this method is that the output scenarios are correlated with the data from the prior month. As a result, the quality of the derived solution using stochastic optimization is highly dependent on the scenario instants that occurred in the previous month.

The second benchmark strategy is based on the ARIMA forecasting method. We forecast each uncertain parameter for the following day.

The standard deviation of forecasting errors can then be calculated. Using the forecasted value and the standard deviation of forecast errors, we generate a large number of scenarios, for example, 1000. Finally, we use the K-Means method to cluster the generated scenarios into a small number, and the centers of the clusters are used to represent the reduced output scenarios. The disadvantage of this strategy is that the temporal correlation is not reflected in the output scenarios, resulting in scenarios that are unduly optimistic and unrealistic.

5 Validation of day-ahead and real-time optimization using test bench and scenarios in numerical environment

The test bench for validating the performance of proposed mathematical formulation is La Chapelle case study, which is a real LV three-phase radial distribution network (230/400 V, 50 Hz) located in a rural area in Switzerland. This network is depicted in Figure 6.

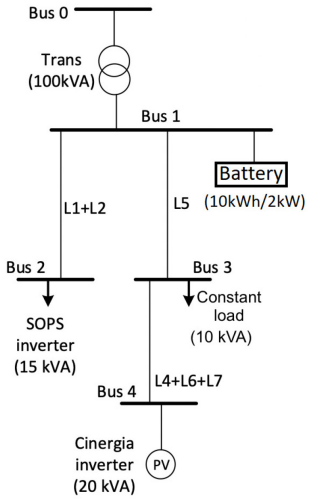

Figure 6: La Chapelle case study.

To run the test, we emulate this network in ReIne laboratory at HEIG-VD [12]. Its electric grid is connected to the transmission system and can emulate a great number of topologies in order to test smart grids control methods. This test grid takes advantage of the flexible and non-flexible generators and demands as well as energy storages connected through bidirectional inverters.

The parameters of the cables in ReIne laboratory are given in Table 4. In addition, the current profiles of different branches and voltage magnitudes of different nodes for the main scenario before and after implementing the set-points of stochastic programming are given in figures 7 and 8. It is worth mentioning that in the ReIne laboratory at HEIG-VD, each line can be emulated by a set of cables in series. For example, the line between buses 1 and 2 is composed of cables L1 and L2 in series. Here, the test is run for 37 time steps, each time step has the duration of 10 minutes. Thus, the total test is run for 6 hours and 10 minutes.

Table 4: The parameters of ReIne laboratory network

	R_U (Ω)	R_V (Ω)	R_W (Ω)	L_U (Ω)	L_V (Ω)	L_W (Ω)
Trans	0.0341	0.0341	0.0341	$7.3e-5$	$7.3e-5$	$7.3e-5$
L1	0.00019	0.00019	0.00019	0.00019	0.00019	0.00019
L2	0.00019	0.00021	0.00020	0.00019	0.00020	0.00020
L4	0.00019	0.00019	0.00019	0.00019	0.00019	0.00020
L5	0.00019	0.00020	0.00021	0.00019	0.00020	0.00019
L6	0.00021	0.00021	0.00020	0.00020	0.00020	0.00020

L7	0.00021	0.00021	0.00020	0.00020	0.00020	0.00020

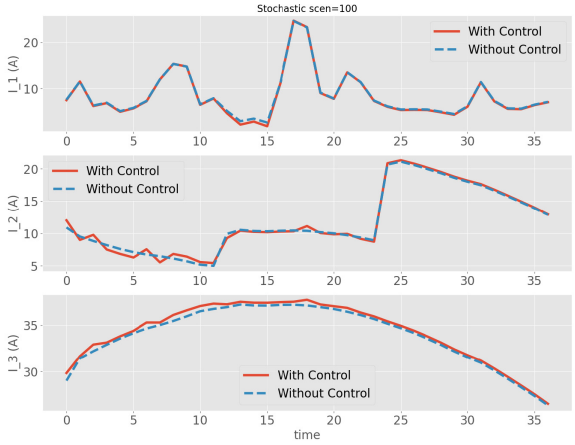

Figure 7: Currents over different lines (I_1 is current of L1+L2, I_2 is current of L5, I_3 is current of L4+L6+L7).

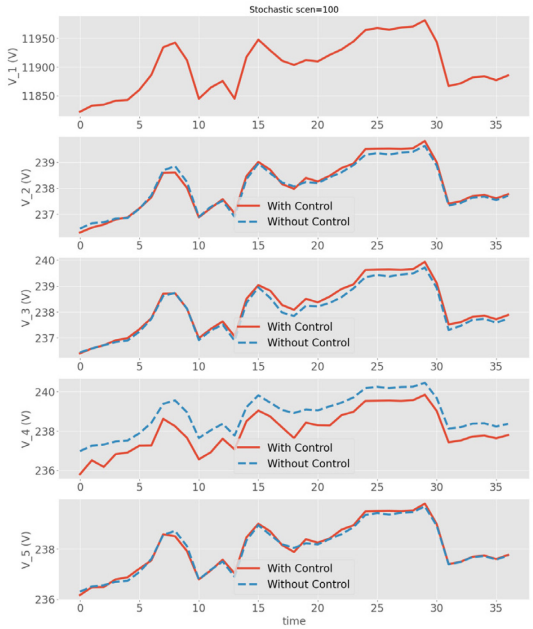

Figure 8: Voltages of different nodes (V_1 is Bus0, V_2 is Bus1, V_3 is Bus2, V_3 is Bus3, V_4 is Bus4).

We solved both pre-scheduling and on-line optimization problem. We consider the uncertainties of PVs production, active/reactive power of demands, and voltage magnitudes of connection point as below

$$\underline{\zeta_{nt}^{(V)}} = \overline{\zeta_{nt}^{(V)}} = 600V,$$

$$\underline{\zeta_{dt}^{(P,DEM)}} = \overline{\zeta_{dt}^{(P,DEM)}} = 0.1 \times P_{dt0}^{(DEM)},$$

$$\underline{\zeta_{dt}^{(Q,DEM)}} = \overline{\zeta_{dt}^{(Q,DEM)}} = 0.1 \times Q_{dt0}^{(DEM)},$$

$$\underline{\zeta_{it}^{(PV)}} = \overline{\zeta_{it}^{(PV)}} = 0.2 \times P_{it0}^{(PV)}.$$

The following 7 models are compared/validated:

- Model 1: stochastic programming with 100 in-sample scenarios,
- Model 2: distributionally robust programming with confidence-level, i.e., $1 - e$, equal to 0.75,
- Model 3: distributionally robust programming with confidence-level, i.e., $1 - e$, equal to 0.85,
- Model 4: distributionally robust programming with confidence-level, i.e., $1 - e$, equal to 0.90,
- Model 5: distributionally robust programming with confidence-level, i.e., $1 - e$, equal to 0.95,
- Model 6: distributionally robust programming with confidence-level, i.e., $1 - e$, equal to 0.97,
- Model 7: distributionally robust programming with confidence-level, i.e., $1 - e$, equal to 1.00.

The active/reactive power at connection point and the offers to the markets for these 7 models are given in figures 9-15.

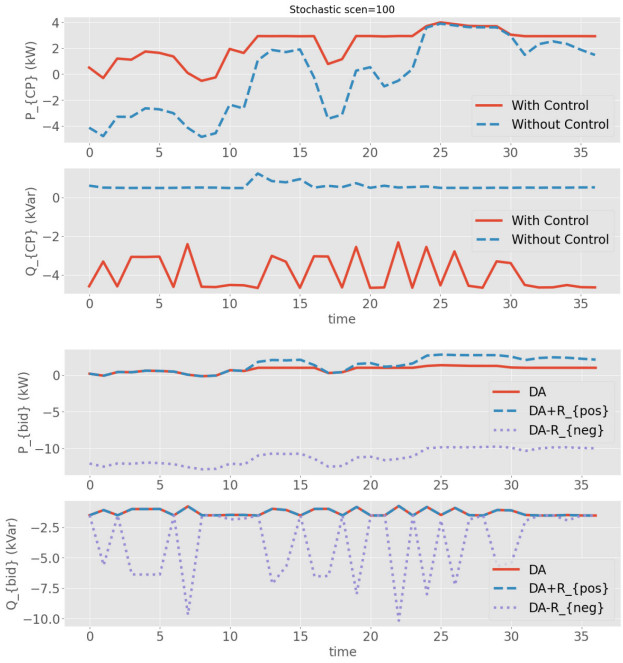

Figure 9: Active/reactive power at connection point and offered energy and flexibilities to the upper layer grid (Model 1).

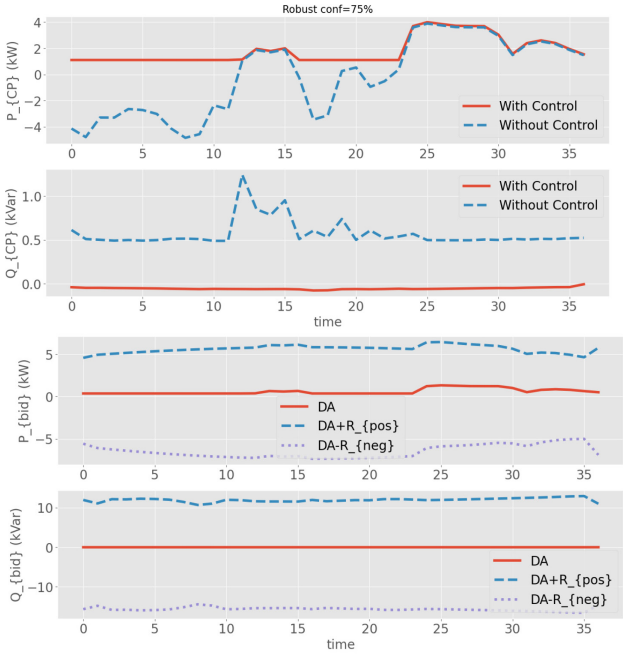

Figure 10: Active/reactive power at connection point and offered energy and flexibilities to the upper layer grid (Model 2).

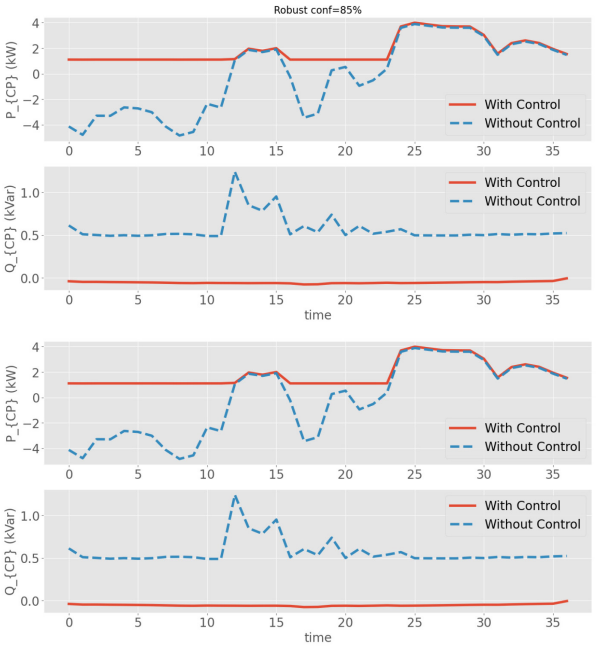

Figure 11: Active/reactive power at connection point and offered energy and flexibilities to the upper layer grid (Model 3).

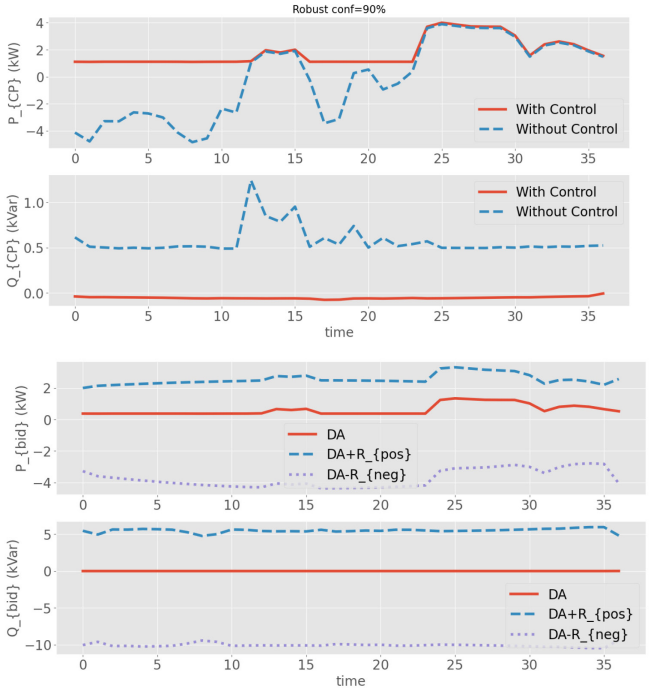

Figure 12: Active/reactive power at connection point and offered energy and flexibilities to the upper layer grid (Model 4).

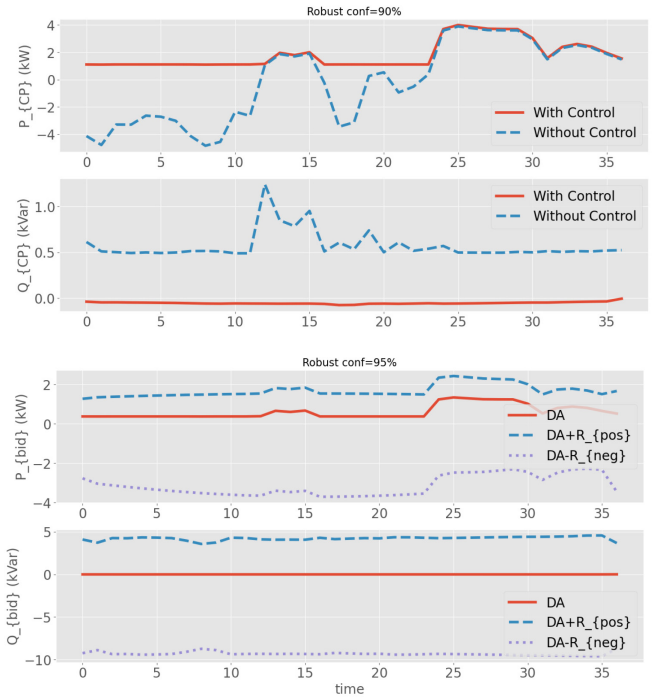

Figure 13: Active/reactive power at connection point and offered energy and flexibilities to the upper layer grid (Model 5).

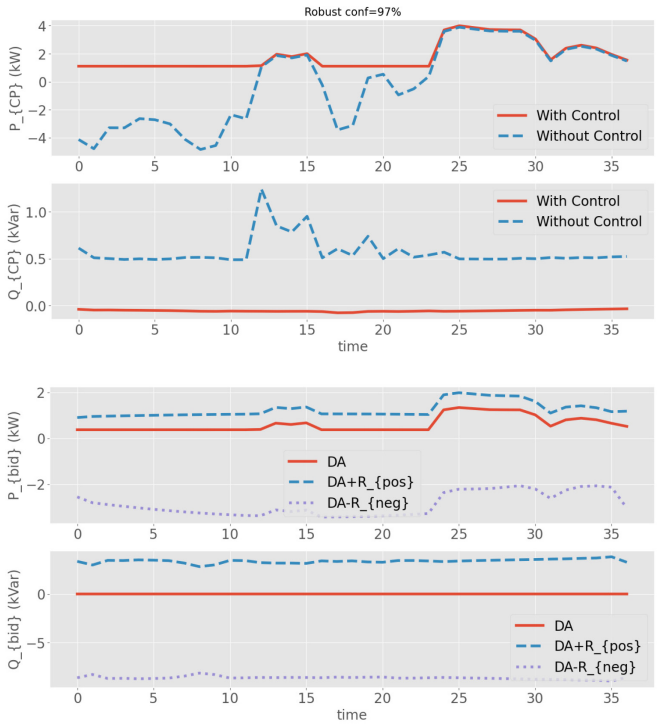

Figure 14: Active/reactive power at connection point and offered energy and flexibilities to the upper layer grid (Model 6).

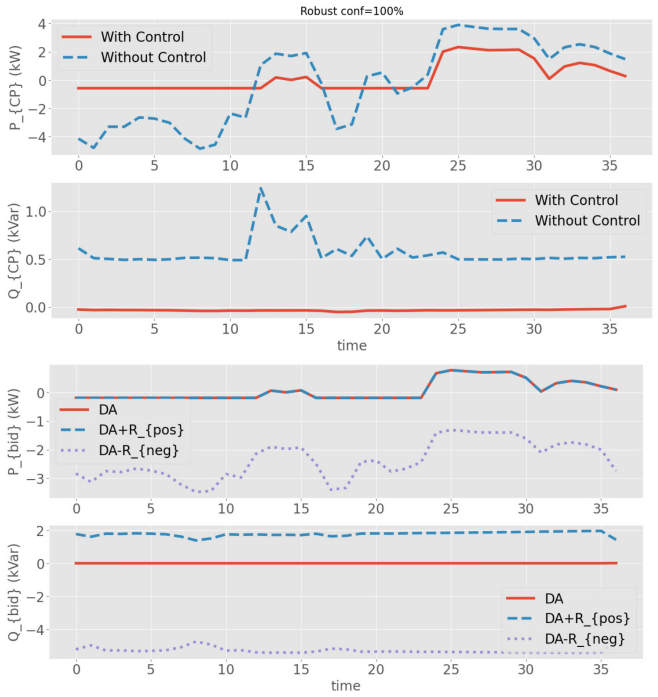

Figure 15: Active/reactive power at connection point and offered energy and flexibilities to the upper layer grid (Model 7).

By comparing the results of these models, the following conclusions can be made:

- By increasing the confidence-level in distributionally robust programming, the amount of positive active power flexibility will be reduced while the amount of negative active power flexibility is not changed too much. The reason behind this is that the resources for positive flexibility is limited.
- In case of stochastic programming, more active power is sold to the upper layer. It is because we need more than 100 scenarios to represent the existing uncertainties in the system.
- The result of distributionally robust programming is more conservative because of the nature of the formulation. By decreasing the confidence-level of the output, i.e., $1-e$, we can obtain a less conservative solution.

The resulted income implementing these 7 models are compared in Figure 16. As one can see by selecting appropriate confidence-level, the income will not be decreased too much, while the solution becomes more robust against existing uncertainties. Here, the prices are considered as below.

$$\lambda_{nt}^{(P)}.P_{nt}^{(SC)} = 100, \lambda_{nt}^{(P+)} = \lambda_{nt}^{(P-)} = 10$$
$$\lambda_{nt}^{(Q)} = \lambda_{nt}^{(Q+)} = \lambda_{nt}^{(Q-)} = 0$$

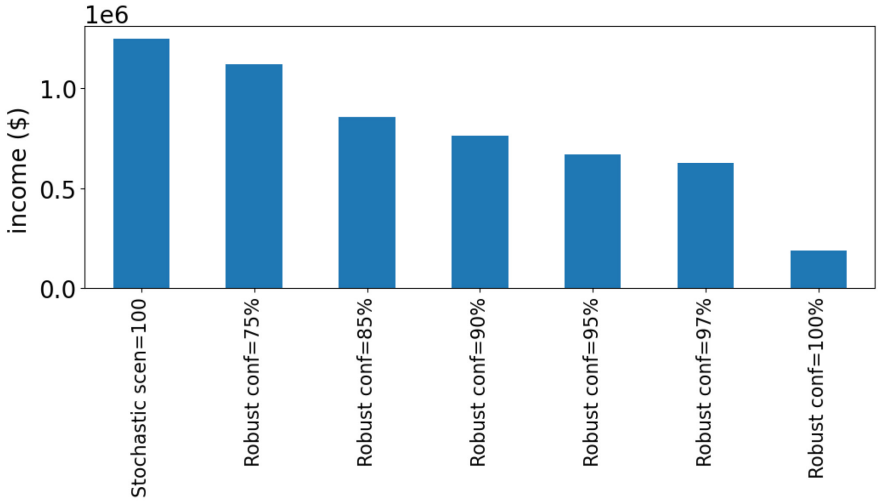

Figure 16: Comparison of 7 models in pre-scheduling optimization with regard to the resulted incomes.

For all these 7 models, we generate 100 out-of-sample scenarios and we use the methodology of Monte-Carlo simulation. At each time step and each out-of-sample scenario, we solve the on-line optimization problem. Then, we find the number of time steps in each scenario that we deviated from the schedules of prescheduling problem and the commands of upper layer grid system operator. We illustrate the box diagram of deviation probability for these scenarios in Figure 17.

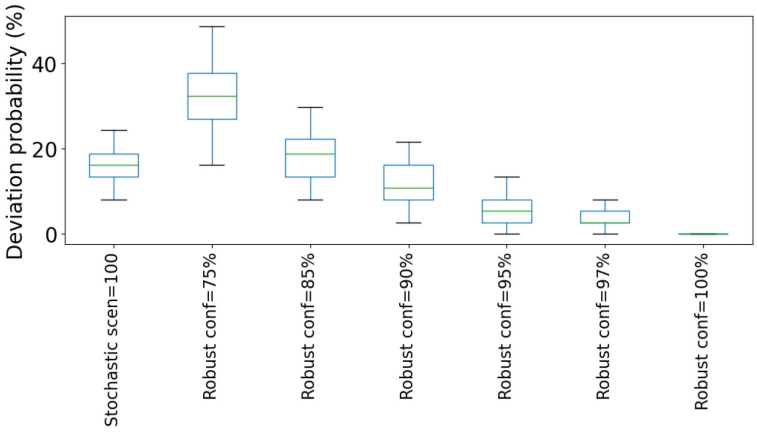

Figure 17: Comparison of 7 models in pre-scheduling optimization with regard to the deviation probabilities in out-of-sample scenarios.

As one can see that the stochastic programming has the similar deviation probability compared to the case where the confidence-level is 0.85. The only difference is that the stochastic programming needs more computational time and data. By increasing the confidence-level, we can obtain better performance with regard to the deviation probability while we sacrifice the income at day-ahead market. The regulation of upper layer grid operator can determine the value of confidence-level.

6 Validation of Markov Chain model using test bench and scenarios in numerical environment

For August 27th, 2021, the proposed stochastic optimization problem and developed data-driven scenario selection strategy are used to plan and exploit the underlying flexibilities. The last 30 days of demanded real power and PV power production data are shown in Figure 18. Similar figures can be plotted for other uncertain parameters.

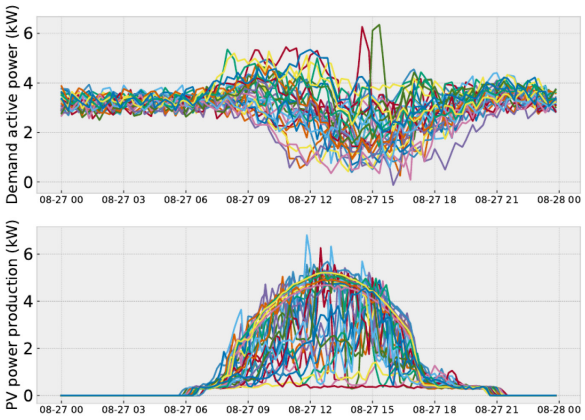

Figure 18: The actual data from the previous 30 days (each color presents data in one day with 10 minutes resolution).

We apply the proposed scenario selection strategy and the mentioned two benchmarks in Python using the packages “sklearn”, “scipy”, and “quantecon”. The results of the first and second benchmarks with K=3. We can choose a greater number of K and analyze the solution's sensitivity to this number. The results are shown in Figures 19 and 20, respectively. Furthermore, the result of proposed strategy with K=3 is shown in Figure 21.

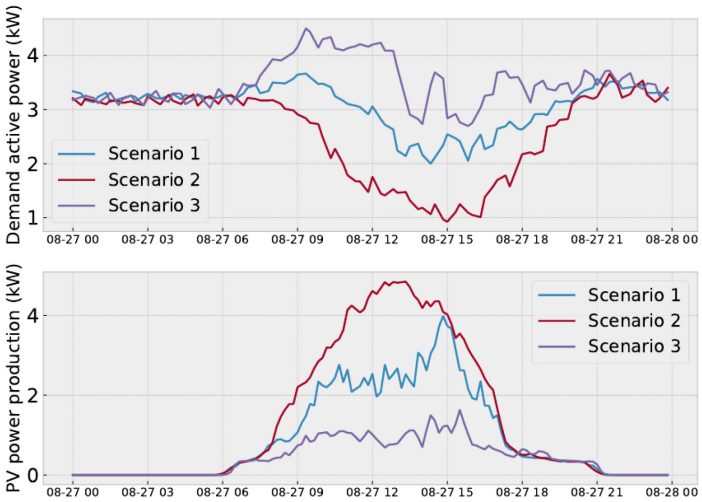

Figure 19: Generated scenarios using the first benchmark strategy.

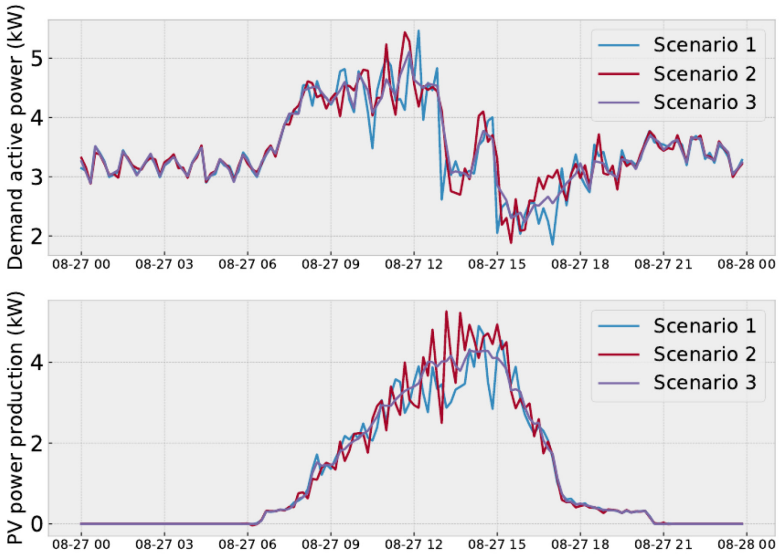

Figure 20: Generated scenarios using the second benchmark strategy.

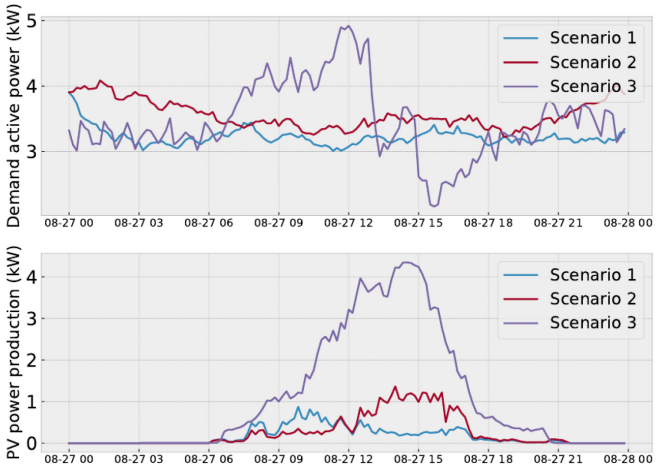

Figure 21: Generated scenarios using the proposed strategy.

By comparing the figures' results, it can be seen that the first benchmark's outcome is correlated to the actual data from the previous 30 days. Because the patterns of electricity demand and PV power production capability during the day are similar for different scenarios, the resulting cluster centres show similar behaviour for uncertain parameters. Furthermore, the second benchmark's result includes three quite identical scenarios in which the temporal correlation is neglected, resulting in scenarios that are unlikely to be experienced in practice. The proposed scenario selection strategy in Figure 21, on the other hand, leads to a more realistic perspective on the general behaviour of the uncertain parameters. This is because the proposed scenario selection strategy solely utilize the data from the previous month related to the forecast.

We can deduce the following from the figures:

- The proposed scenario selection strategy generates a number of realistic scenarios, making the result robust to the uncertainties. As a result, the objective is reduced as expected for the advantage of robustness against uncertainties.
- The first benchmark considers operating scenarios that are similar. As a result, a significant amount of reactive power flexibility has been miss-planned.
- The second benchmark model is even more optimistic, and as a result, we wrongly assumed we could consume less between 14:00 and 18:00.
- Because the prices for upward and downward reactive power flexibilities are the same and the price for producing/consuming reactive power is zero, the planned reactive power becomes so volatile in Figures 19, 20, and 21.
- Although the outputs of the proposed strategy and the first benchmark appear to be quite similar, there is a significant difference in the objectives. This is due to the fact that the scenarios generated by the first benchmark have a high correlation with the data from the previous month.

7 Conclusion

In this report, the formulation of pre-scheduling and on-line optimization problems are presented that can be used for flexibility provision by resources in distribution grids. The advantages of using distributionally robust optimization instead of stochastic programming for pre-scheduling problem have been justified. In distribution grid, as the data for producing exact probability distribution functions of uncertainties is not available and we can have only the boundary of uncertainties, distributionally robust optimization is applicable. In addition, the solution of distributionally robust optimization is not so conservative. By tuning the parameter of confidence-level in distributionally robust optimization, we can compromise between the optimality and robustness of the solution against uncertainties. The performance of proposed formulation is evaluated using a numerical case study. One can see that by increasing the confidence-level, a better performance can be obtained with regard to the deviation probability while the income at day-ahead market will be sacrificed. By increasing the confidence-level, the amount of positive active power flexibility is also reduced while the amount of negative active power flexibility is not changed too much.

The case study of Markov chains compares the efficiency of the proposed scenario selection strategy to conventional methods, i.e., those based on real-world data and ARIMA forecasting. The proposed formulation's computational complexity is significantly reduced, while a number of robust constraints are established. The final stochastic optimization problem is scalable and can be used in ADNs with a large number of buses, which is an advantage of this method over using a large number of scenarios.

8 Appendix A

First, we write the uncertain parameters $|V_{nt\omega}|: n \in \mathbb{N}^{(TC)}$, $P_{dt\omega}^{(DEM)}$, $Q_{dt\omega}^{(DEM)}$, $P_{it\omega}^{(PV,max)}$, $r_{nt\omega}^{(RT,P)}$, and $r_{nt\omega}^{(RT,Q)}$ as follows:

$$|V_{nt\omega}| = |V_{n0}^{(base)}| + \zeta_{nt\omega}^{(V)}; \forall n \in \mathbb{N}^{(TC)}, \tag{92}$$

$$P_{dt\omega}^{(DEM)} = P_{dt0}^{(DEM)} + \zeta_{dt\omega}^{(P,DEM)}; \forall d \in \mathbb{D}, \tag{93}$$

$$Q_{dt\omega}^{(DEM)} = Q_{dt0}^{(DEM)} + \zeta_{dt\omega}^{(Q,DEM)}; \forall d \in \mathbb{D}, \tag{94}$$

$$P_{it\omega}^{(PV,max)} = P_{it0}^{(PV,max)} + \zeta_{it\omega}^{(PV)}; \forall i \in \mathbb{I}, \tag{95}$$

$$r_{nt\omega}^{(RT,P)} = 0 + \zeta_{nt\omega}^{(RT,P)}; \forall n \in \mathbb{N}^{(TC)}, \tag{96}$$

$$r_{nt\omega}^{(RT,Q)} = 0 + \zeta_{nt\omega}^{(RT,Q)}; \forall n \in \mathbb{N}^{(TC)}, \tag{97}$$

where scenario 0 represents the forecasted magnitude of uncertain parameters and

$$\zeta_{nt\omega}^{(V)} \in [-\underline{\zeta_{nt}^{(V)}}, \overline{\zeta_{nt}^{(V)}}], \tag{98}$$

$$\zeta_{dt\omega}^{(P,DEM)} \in [-\underline{\zeta_{dt}^{(P,DEM)}}, \overline{\zeta_{dt}^{(P,DEM)}}], \tag{99}$$

$$\zeta_{dt\omega}^{(Q,DEM)} \in [-\underline{\zeta_{dt}^{(Q,DEM)}}, \overline{\zeta_{dt}^{(Q,DEM)}}], \tag{100}$$

$$\zeta_{it\omega}^{(PV)} \in [-\underline{\zeta_{it}^{(PV)}}, \overline{\zeta_{it}^{(PV)}}], \tag{101}$$

$$\zeta_{nt\omega}^{(RT,P)} \in [-R_{nt}^{(SC,P-)}, R_{nt}^{(SC,P+)}], \tag{102}$$

$$\zeta_{nt\omega}^{(RT,Q)} \in [-R_{nt}^{(SC,Q-)}, R_{nt}^{(SC,Q+)}], \tag{103}$$

represent the forecast errors.

Second, the constraints (75)-(78) are included in the pre-scheduling problem just for the forecasted scenario, i.e., $\omega = 0$, and values of $|V_{n0}^{(base)}|: \forall n \in \mathbb{N}^{(TC)}$, $P_{dt0}^{(DEM)}$, $Q_{dt0}^{(DEM)}$, $P_{it0}^{(PV,max)}$, $r_{nt0}^{(RT,P)}(=0)$, and $r_{nt0}^{(RT,Q)}(=0)$.

Third, the maximum and minimum amounts of active and reactive power deviations are calculated as below.

$$\zeta_{net}^{(P+)} = \sum_{n\in\mathbb{N}^{(TC)}} R_{nt}^{(SC,P+)} + \sum_{d\in\mathbb{D}} \overline{\zeta_{dt}^{(P,DEM)}} - \sum_{i\in\mathbb{I}} \underline{\zeta_{it}^{(PV)}}, \tag{104}$$

$$\zeta_{net}^{(P-)} = \sum_{n\in\mathbb{N}^{(TC)}} R_{nt}^{(SC,P-)} + \sum_{d\in\mathbb{D}} \underline{\zeta_{dt}^{(P,DEM)}} - \sum_{i\in\mathbb{I}} \overline{\zeta_{it}^{(PV)}}, \tag{105}$$

$$\zeta_{net}^{(Q+)} = \sum_{n\in\mathbb{N}^{(TC)}} R_{nt}^{(SC,Q+)} + \sum_{d\in\mathbb{D}} \overline{\zeta_{dt}^{(Q,DEM)}}, \tag{106}$$

$$\zeta_{net}^{(Q-)} = \sum_{n\in\mathbb{N}^{(TC)}} R_{nt}^{(SC,Q-)} + \sum_{d\in\mathbb{D}} \underline{\zeta_{dt}^{(Q,DEM)}}. \tag{107}$$

Fourth, the maximum/minimum magnitudes of outputs of PVs, BESSs, and real-time active/reactive power injection at connection points are estimated as below:

$$\overline{P_{it}^{(PV)}} = P_{it0}^{(PV)} + \overline{\zeta_{it}^{(PV)}} + \alpha_{it}^{(PV,P+)}; \forall i \in \mathbb{I}, \tag{108}$$

$$\underline{P_{it}^{(PV)}} = P_{it0}^{(PV)} - \underline{\zeta_{it}^{(PV)}} - \alpha_{it}^{(PV,P-)}; \forall i \in \mathbb{I}, \tag{109}$$

$$\overline{Q_{it}^{(PV)}} = Q_{it0}^{(PV)} + \alpha_{it}^{(PV,Q+)}; \forall i \in \mathbb{I}, \tag{110}$$

$$\underline{Q_{it}^{(PV)}} = Q_{it0}^{(PV)} - \alpha_{it}^{(PV,Q-)}; \forall i \in \mathbb{I}, \tag{111}$$

$$\overline{P_{st}^{(BESS)}} = P_{st0}^{(BESS)} + \alpha_{st}^{(BESS,P+)}; \forall s \in \mathbb{S}, \tag{112}$$

$$\underline{P_{st}^{(BESS)}} = P_{st0}^{(BESS)} - \alpha_{st}^{(BESS,P-)}; \forall s \in \mathbb{S}, \tag{113}$$

$$\overline{Q_{st}^{(BESS)}} = Q_{st0}^{(BESS)} + \alpha_{st}^{(BESS,Q+)}; \forall s \in \mathbb{S}, \tag{114}$$

$$\underline{Q_{st}^{(BESS)}} = Q_{st0}^{(BESS)} - \alpha_{st}^{(BESS,Q-)}; \forall s \in \mathbb{S}, \tag{115}$$

$$\overline{P_{nt}^{(RT)}} = P_{nt}^{(SC)} - \alpha_{nt}^{(RT,P+)}; \forall n \in \mathbb{N}^{(TC)}, \tag{116}$$

$$\underline{P_{nt}^{(RT)}} = P_{nt}^{(SC)} + \alpha_{nt}^{(RT,P-)}; \forall n \in \mathbb{N}^{(TC)}, \tag{117}$$

$$\overline{Q_{nt}^{(RT)}} = Q_{nt}^{(SC)} - \alpha_{nt}^{(RT,Q+)}; \forall n \in \mathbb{N}^{(TC)}. \tag{118}$$

$$\underline{Q_{nt}^{(RT)}} = Q_{nt}^{(SC)} + \alpha_{nt}^{(RT,Q-)}; \forall n \in \mathbb{N}^{(TC)}. \tag{119}$$

here $\alpha_{it}^{(PV,P+)}$, $\alpha_{it}^{(PV,P-)}$, $\alpha_{it}^{(PV,Q+)}$, $\alpha_{it}^{(PV,Q-)}$, $\alpha_{st}^{(BESS,P+)}$, $\alpha_{st}^{(BESS,P-)}$, $\alpha_{st}^{(BESS,Q+)}$, $\alpha_{st}^{(BESS,Q-)}$, $\alpha_{nt}^{(RT,P+)}$, $\alpha_{nt}^{(RT,P-)}$, $\alpha_{nt}^{(RT,Q+)}$, and $\alpha_{nt}^{(RT,Q-)}$ are the participation factors of resources to compensate the uncertainties. Note that the sum of these participation factors is equal to the maximum/minimum amounts of active/reactive power deviations in the grid.

$$\sum_{i\in\mathbb{I}} \alpha_{it}^{(PV,P+)} + \sum_{s\in\mathbb{S}} \alpha_{st}^{(BESS,P+)} + \sum_{n\in\mathbb{N}^{(TC)}} \alpha_{nt}^{(RT,P+)} = \zeta_{net}^{(P+)}; \forall t \in \mathbb{T}, \tag{120}$$

$$\sum_{i\in\mathbb{I}} \alpha_{it}^{(PV,P-)} + \sum_{s\in\mathbb{S}} \alpha_{st}^{(BESS,P-)} + \sum_{n\in\mathbb{N}^{(TC)}} \alpha_{nt}^{(RT,P-)} = \zeta_{net}^{(P-)}; \forall t \in \mathbb{T}, \tag{121}$$

$$\sum_{i\in\mathbb{I}} \alpha_{it}^{(PV,Q+)} + \sum_{s\in\mathbb{S}} \alpha_{st}^{(BESS,Q+)} + \sum_{n\in\mathbb{N}^{(TC)}} \alpha_{nt}^{(RT,Q+)} = \zeta_{net}^{(Q+)}; \forall t \in \mathbb{T}, \tag{122}$$

$$\sum_{i\in\mathbb{I}} \alpha_{it}^{(PV,Q-)} + \sum_{s\in\mathbb{S}} \alpha_{st}^{(BESS,Q-)} + \sum_{n\in\mathbb{N}^{(TC)}} \alpha_{nt}^{(RT,Q-)} = \zeta_{net}^{(Q-)}; \forall t \in \mathbb{T}, \tag{123}$$

Fifth, the maximum and minimum deviation of active/reactive power injections at each node are estimated as

$$\overline{P_{nt}} = P_t^{(+)} - \sum_{i\in\mathbb{I}_n} \alpha_{it}^{(PV,P+)} - \sum_{s\in\mathbb{S}_n} \alpha_{st}^{(BESS,P+)} + \sum_{n'\in\mathbb{N}^{(TC)},n'==n} \alpha_{n't}^{(RT,P+)}; \forall n \in \mathbb{N}, \tag{124}$$

$$\underline{P_{nt}} = P_t^{(-)} - \sum_{i\in\mathbb{I}_n} \alpha_{it}^{(PV,P-)} - \sum_{s\in\mathbb{S}_n} \alpha_{st}^{(BESS,P-)} + \sum_{n'\in\mathbb{N}^{(TC)},n'==n} \alpha_{n't}^{(RT,P-)}; \forall n \in \mathbb{N}, \tag{125}$$

$$\overline{Q_{nt}} = Q_t^{(+)} - \sum_{i\in\mathbb{I}_n} \alpha_{it}^{(PV,Q+)} - \sum_{s\in\mathbb{S}_n} \alpha_{st}^{(BESS,Q+)} + \sum_{n'\in\mathbb{N}^{(TC)},n'==n} \alpha_{n't}^{(RT,Q+)}; \forall n \in \mathbb{N}, \tag{126}$$

$$\underline{Q_{nt}} = Q_t^{(-)} - \sum_{i\in\mathbb{I}_n} \alpha_{it}^{(PV,Q-)} - \sum_{s\in\mathbb{S}_n} \alpha_{st}^{(BESS,Q-)} + \sum_{n'\in\mathbb{N}^{(TC)},n'==n} \alpha_{n't}^{(RT,Q-)}; \forall n \in \mathbb{N}, \tag{127}$$

Sixth, the maximum and minimum values of voltages, currents, and SOC of BESSs are estimated as follows:

$$\bar{V}_{nt} = V_{nt0} + \sum_{n\in\mathbb{N}^{(TC)}} \overline{\zeta_{nt}^{(V)}} + \sum_{n'\in\mathbb{N}} K_{nn'}^{(VP)} \underline{P_{nt}} + \sum_{n'\in\mathbb{N}} K_{nn'}^{(VQ)} \underline{Q_{nt}}; \forall n \in \mathbb{N}, \forall t \in \mathbb{T}, \tag{128}$$

$$\underline{V}_{nt} = V_{nt0} + \sum_{n\in\mathbb{N}^{(TC)}} \underline{\zeta_{n1t}^{(V)}} - \sum_{n'\in\mathbb{N}} K_{nn'}^{(VP)} \overline{P_{nt}} - \sum_{n'\in\mathbb{N}} K_{nn'}^{(VQ)} \overline{Q_{nt}}; \forall n \in \mathbb{N}, \forall t \in \mathbb{T}, \tag{129}$$

$$\bar{I}_{nn't} = I_{nn't0} + + \sum_{n''\in\mathbb{N}} K_{nn'n''}^{(IP)} \overline{P_{nt}} + \sum_{n''\in\mathbb{N}} K_{nn'n''}^{(IQ)} \overline{Q_{nt}}; \forall n \in \mathbb{N}, \forall n' \in \mathbb{N}, \forall t \in \mathbb{T}, \tag{130}$$

$$\overline{\mathrm{SOC}}_{st\omega} = \overline{\mathrm{SOC}}_{st0} + \sum_{t'\le t} \alpha_{st'}^{(BESS,P+)}; \forall s \in \mathbb{S}, \tag{131}$$

$$\underline{\mathrm{SOC}}_{st\omega} = \underline{\mathrm{SOC}}_{st0} - \sum_{t'\le t} \alpha_{st'}^{(BESS,P-)}; \forall s \in \mathbb{S}. \tag{132}$$

Finally, the following chance constraint is added for limiting the deviation of active/reactive power of connection points with respect to the commands of upper layer grid system operator.

$$Prob\Big(\sum_{n\in\mathbb{N}^{(TC)}} \alpha_{nt}^{(f)} \le \delta\Big) \le 1 - e; \forall t \in \mathbb{T}, \forall f \in \{P+, P-, Q+, Q-\}, \tag{133}$$

where δ is a small constant and $1 - e$ is the confidence-level.

9 Appendix B

By using the Chebyshev inequality theorem, the constraint (133) can be replaced by the following one.

$$\sum_{n\in\mathbb{N}^{(TC)}} \alpha_{nt}^{(f)} \leq \frac{(\zeta_{net}^{(f)})^2.\delta}{\zeta_{net}^{(f)} + \Phi^{-1}(1-e).\sigma_{net}^{(f)}}; \forall t \in \mathbb{T}, \forall f \in \{P+, P-, Q+, Q-\}, \tag{134}$$

where, $\Phi^{-1}(1-e)$ is the inverse of cumulative Gaussian function, and $\sigma_{net}^{(f)}$ is calculated as follows:

$$\sigma_{net}^{(P+)} = \sqrt{\sum_{n\in\mathbb{N}^{(TC)}} \left(\frac{R_{nt}^{(SC,P+)}}{\Phi^{-1}(1-\theta_n^{(SC,P)})}\right)^2 + \sum_{d\in\mathbb{D}} \left(\frac{\overline{\zeta_{dt}^{(P,DEM)}}}{\Phi^{-1}(1-\theta_n^{(P,DEM)})}\right)^2 + \sum_{d\in\mathbb{D}} \left(\frac{\zeta_{it}^{(PV)}}{\Phi^{-1}(1-\theta_n^{(PV)})}\right)^2}, \tag{135}$$

$$\sigma_{net}^{(P-)} = \sqrt{\sum_{n\in\mathbb{N}^{(TC)}} \left(\frac{R_{nt}^{(SC,P-)}}{\Phi^{-1}(1-\theta_n^{(SC,P)})}\right)^2 + \sum_{d\in\mathbb{D}} \left(\frac{\zeta_{dt}^{(P,DEM)}}{\Phi^{-1}(1-\theta_n^{(P,DEM)})}\right)^2 + \sum_{d\in\mathbb{D}} \left(\frac{\overline{\zeta_{it}^{(PV)}}}{\Phi^{-1}(1-\theta_n^{(PV)})}\right)^2}, \tag{136}$$

$$\sigma_{net}^{(Q+)} = \sqrt{\sum_{n\in\mathbb{N}^{(TC)}} \left(\frac{R_{nt}^{(SC,Q+)}}{\Phi^{-1}(1-\theta_n^{(SC,Q)})}\right)^2 + \sum_{d\in\mathbb{D}} \left(\frac{\overline{\zeta_{dt}^{(Q,DEM)}}}{\Phi^{-1}(1-\theta_n^{(Q,DEM)})}\right)^2}, \tag{137}$$

$$\sigma_{net}^{(Q-)} = \sqrt{\sum_{n\in\mathbb{N}^{(TC)}} \left(\frac{R_{nt}^{(SC,Q-)}}{\Phi^{-1}(1-\theta_n^{(SC,Q)})}\right)^2 + \sum_{d\in\mathbb{D}} \left(\frac{\zeta_{dt}^{(Q,DEM)}}{\Phi^{-1}(1-\theta_n^{(Q,DEM)})}\right)^2}. \tag{138}$$

However, while constraints (135)-(135) can be integrated in a SOCP problem, constraint (134) is non-convex. For convexifying that, we estimate the right-hand side of (134) as below:

$$\frac{(\zeta_{net}^{(f)})^2.\delta}{\zeta_{net}^{(f)} + \Phi^{-1}(1-e).\sigma_{net}^{(f)}} \approx (\zeta_{net}^{(f)} - \Phi^{-1}(1-e).\sigma_{net}^{(f)}).\delta + \delta; \forall f \in \{P+, P-, Q+, Q-\}. \tag{139}$$

The accuracy of this approximation is high for value of e close to zero.

10 Bibliography

[1] Farivar, Masoud, and Steven H. Low. "Branch flow model: Relaxations and convexification—Part I." IEEE Transactions on Power Systems 28, no. 3 (2013): 2554-2564.

[2] Nick, Mostafa, Rachid Cherkaoui, Jean-Yves Le Boudec, and Mario Paolone. "An exact convex formulation of the optimal power flow in radial distribution networks including transverse components." IEEE Transactions on Automatic Control 63, no. 3 (2017): 682-697.

[3] Christakou, Konstantina, Jean-Yves LeBoudec, Mario Paolone, and Dan-Cristian Tomozei. "Efficient computation of sensitivity coefficients of node voltages and line currents in unbalanced radial electrical distribution networks." IEEE Transactions on Smart Grid 4, no. 2 (2013): 741-750.

[4] Bozorg, Mokhtar, Omid Alizadeh-Mousavi, Sebastien Wasterlain, and Mauro Carpita. "Model-less/measurement-based computation of voltage sensitivities in unbalanced electrical distribution networks: experimental validation." In 2019 21st European Conference on Power Electronics and Applications (EPE'19 ECCE Europe), pp. P-1. IEEE, 2019.

[5] Carpita, Mauro, Douglas Houmard, Daniel Siemaszko, Sébastien Wasterlain, Mokhtar Bozorg, Alexandre Karlov, Jean-Roland Schuler et al. SMILE-FA. No. REPORT_SBM. Swiss Federal Office of Energy SFOE, 2018.

[6] Nick, Mostafa, Mokhtar Bozorg, Rachid Cherkaoui, and Mario Paolone. "A Robust Optimization Framework for the Day-Ahead Scheduling of Active Distribution Networks including Energy Storage Systems." In 2019 IEEE Milan PowerTech, pp. 1-6. IEEE, 2019.

[7] Kalantar-Neyestanaki, Mohsen, Fabrizio Sossan, Mokhtar Bozorg, and Rachid Cherkaoui. "Characterizing the Reserve Provision Capability Area of Active Distribution Networks: A Linear Robust Optimization Method." IEEE Transactions on Smart Grid 11, no. 3 (2019): 2464-2475.

[8] Cabrera-Tobar, Ana, Eduard Bullich-Massagué, Mònica Aragüés-Peñalba, and Oriol Gomis-Bellmunt. "Capability curve analysis of photovoltaic generation systems." Solar Energy 140 (2016): 255-264.

[9] Margellos, Kostas, Paul Goulart, and John Lygeros. "On the road between robust optimization and the scenario approach for chance constrained optimization problems." *IEEE Transactions on Automatic Control* 59, no. 8 (2014): 2258-2263.

[10] Gorissen, Bram L., İhsan Yanıkoğlu, and Dick den Hertog. "A practical guide to robust optimization." *Omega* 53 (2015): 124-137.

[11] Wagner, Michael R. "Stochastic 0–1 linear programming under limited distributional information." *Operations Research Letters* 36, no. 2 (2008): 150-156.

[12] Mauro Carpita, Jean-François Affolter, Massimiliano Capezzali, "Relever les défis de la transition énergétique", Bulletin SEV/VSE 10/2018, pp. 39-43, 2018.

[13] Li, Jinghua, Jiasheng Zhou, and Bo Chen. "Review of wind power scenario generation methods for optimal operation of renewable energy systems." *Applied Energy* 280 (2020): 115992.

[14] Kalantar-Neyestanaki, Mohsen, Fabrizio Sossan, Mokhtar Bozorg, and Rachid Cherkaoui. "Characterizing the reserve provision capability area of active distribution networks: A linear robust optimization method." *IEEE Transactions on Smart Grid* 11, no. 3 (2019): 2464-2475.

[15] Kalantar-Neyestanaki, Mohsen, and Rachid Cherkaoui. "Coordinating Distributed Energy Resources and Utility-Scale Battery Energy Storage System for Power Flexibility Provision Under Uncertainty." *IEEE Transactions on Sustainable Energy* 12, no. 4 (2021): 1853-1863.

[16] Campi, Marco C., and Simone Garatti. "The exact feasibility of randomized solutions of uncertain convex programs." *SIAM Journal on Optimization* 19, no. 3 (2008): 1211-1230.

[17] Bolognani, Saverio, and Florian Dörfler. "Fast scenario-based decision making in unbalanced distribution networks." In *2016 Power Systems Computation Conference (PSCC)*, pp. 1-7. IEEE, 2016.